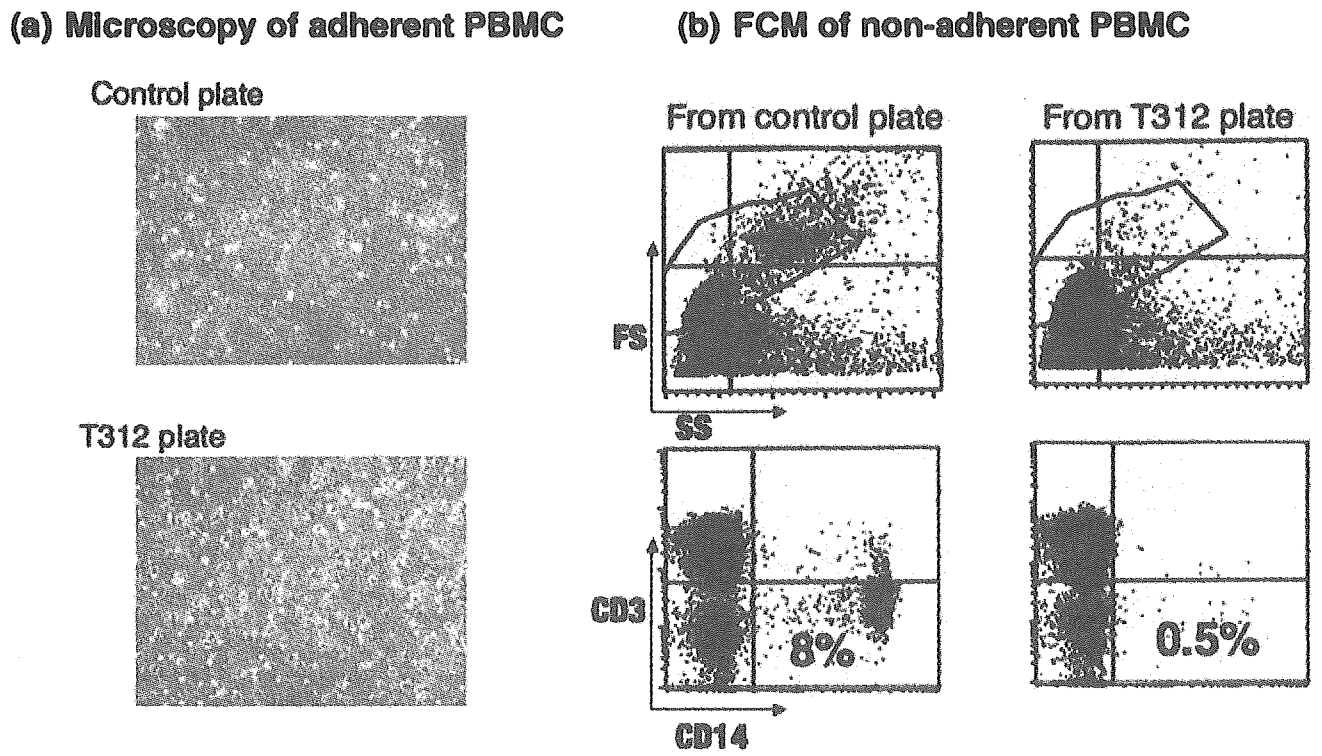

Figure 1. Stable adhesion of monocytes onto the bottom of plastic wells precoated with an anti-human CCR5 mAb. Aliquots (1 ml) of PBMCs at 2×10^6/ml of 5% FCS-RPMI medium were cultured overnight in individual wells of a 12-well plate that had been previously coated either with clone T312 rat IgG1 anti-human CCR5 or an isotype control mAb. (a) The morphology of the adherent cells as seen by phase-contrast microscopy at ×100. (b) Nonadherent PBMCs from each well were collected and analyzed by flow cytometry. The percentages of $CD14^+$ monocytes in the lymphocyte and monocyte gate in nonadherent PBMCs are noted in the double-staining profile with anti-CD3 and anti-CD14 mAbs. FS, forward scatter; SS, side scatter.

directly into the spleen, followed 7 days later with the ip injection of the same number and source of DCs pulsed with the same antigen. Five days later, the mice were sacrificed, and blood was collected by cardiocentesis and human lymphocytes were recovered from both the peritoneal cavity and the spleen. The immune sera were assayed for human antibody titers against OVA or KLH by ELISA using peroxidase-labeled goat anti-human IgG, as described previously (16). For the measurement of antigen-specific human T-cell immune responses, the human lymphocytes (2×10^6 cells) collected from the immunized mice were cultured for 2 days at 37°C in a 5% CO_2 humidified incubator with 2×10^5 autologous APCs (adherent PBMCs) in the presence or absence of either 5 μg/ml OVA or KLH in a volume of 0.5 ml in individual wells of a 24-well microtiter plate (BD Pharmingen). Media used consisted of RPMI medium supplemented with 20 U/ml of IL-2. The concentration of human IFN-γ produced in the culture supernatants was determined by standard ELISA.

Results

1. Cross-Linked CCR5 Induces Strong Adhesion of Monocytes. Twelve-well microtiter plates were first coated with the rat anti-human CCR5 N-terminus antibody (IgG1, clone T312) or an isotype control mAb. Then, PBMCs (5×10^6/ml) isolated from several normal donors were individually incubated overnight at 37°C in a 5% CO_2 humidified incubator in a volume of 1 ml of RPMI medium in each well of the plate. Following incubation, the nonadherent cells were removed. As shown in Figure1a, there appeared to be a marked increase in the number of cells that remained adherent to the wells precoated with the T312 mAb as compared with the control wells. As seen in Figure 1b, of interest was the finding that the nonadherent cells from the T312 mAb-coated wells were selectively depleted of $CD14^+$ cells (0.5%), compared with the nonadherent cells from the control wells (8%). The input unfractionated PBMCs from the various donors used for this study contained levels of $CD14^+$ cells that were essentially similar to the levels noted in the control wells, indicating that incubation of the PBMCs in the T312 precoated wells led to the select adhesion of the $CD14^+$ cells. Lymphoid cells other than $CD14^+$ monocytes were also present in the population of cells that adhered to the T312 mAb-coated wells, which mainly consisted of T and B cells, constituting up to 20% of the total adherent cells (data not shown). It is important to note that the addition of the T312 mAb to aliquots of the PBMCs from the same donors before incubation in the microtiter wells or the addition of the same T312 mAb to the PBMCs following dispensing of the cells

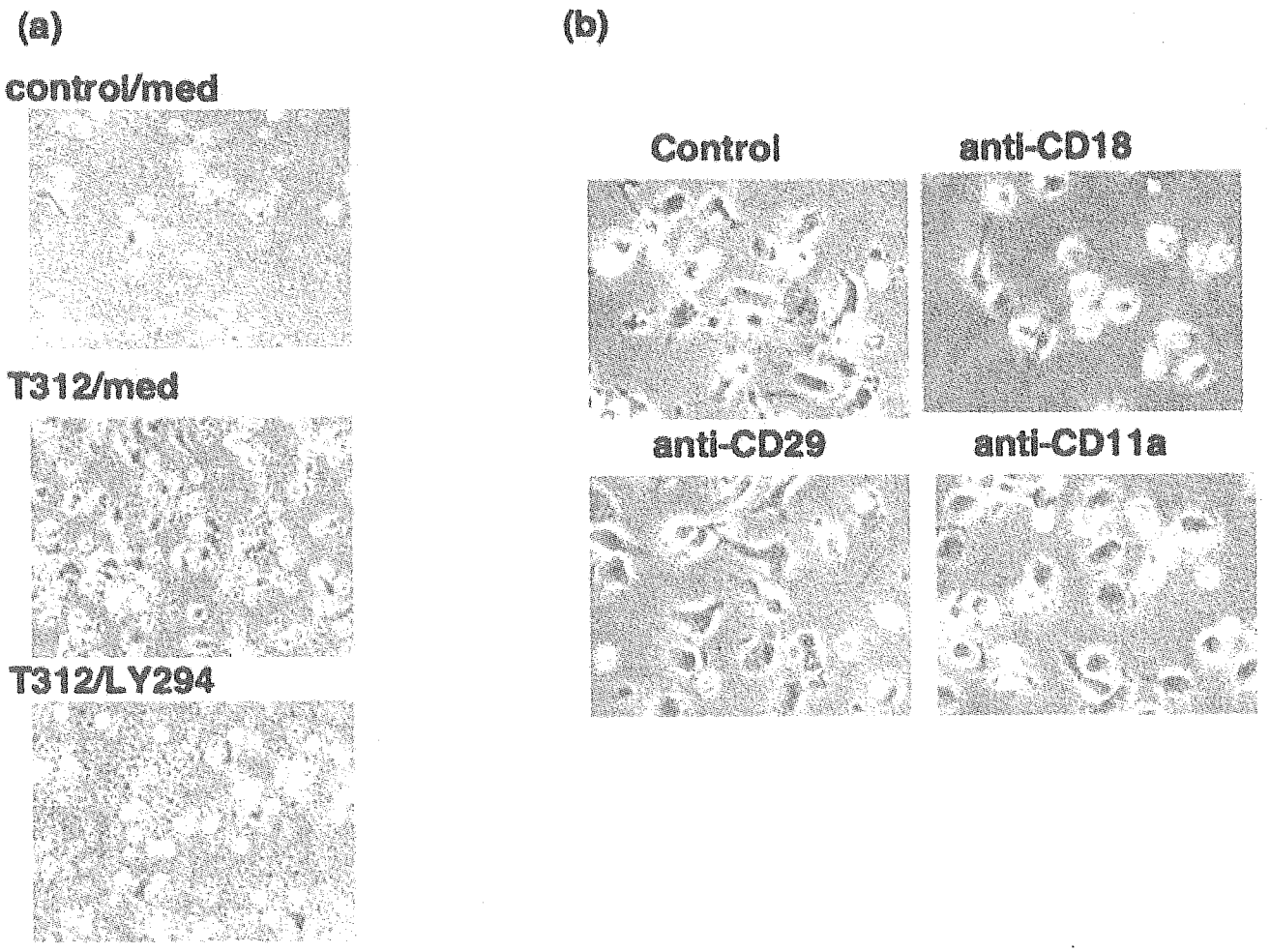

Figure 2. Microscopic analysis of the mechanisms for monocyte adhesion following CCR5 cross-linking. (a) PBMCs were incubated for 2 hrs in control mAb-coated wells (control/med) or overnight in T312 mAb-coated wells in medium alone (T312/med) or in the presence or of 5 μ*M* PI3-K inhibitor, LY294.002 (T312/LY294). (b) PBMCs were cultivated overnight in T312 mAb-coated wells in medium alone (control) or in the presence of 10 μg/ml of each mAb: anti-CD18, CD29, or CD11a. In these experiments, nonadherent cells were removed by gentle washing, and the wells were analyzed microscopically at ×200.

into the microtiter wells did not lead to increased adhesion of the $CD14^+$ monocytes, providing evidence indicating that the antibody had to be cross-linked for the adhesion to occur. A study of the kinetics of cell adhesion to the T312 mAb-coated wells was also performed. It should also be noted that there was a difference in the incubation time for maximal yield of monocytes following incubation of PBMCs in wells precoated with the T312 mAb, compared with the control antibody. Thus, where a 2-hr incubation was sufficient to obtain the maximum yield of monocytes by incubation of PBMCs in the control antibody-coated wells, it required an overnight or 24-hr incubation in the T312 mAb-coated wells (data not shown). Thus, for all further studies, adherent cells were isolated by incubation of the PBMCs either for 2 hrs in control wells or overnight in T312 mAb-coated wells, unless otherwise noted.

Since binding of CCR5 by its natural ligands is known to induce intracellular signaling via the PI3-K pathway, experiments were carried out to determine if such signaling was a prerequisite for the stable binding of the monocytes to the T312 mAb-coated wells. The above experiment was repeated, with the only difference being that an aliquot of each of the donor PBMCs was incubated in the T312 mAb-coated wells in the presence of 5 μ*M* of the PI3-K inhibitor LY294.002. Representative data shown in Figure 2a demonstrate that the addition of the PI3-K inhibitor completely blocked the cell adhesion. Flow cytometric analysis of the nonadherent cells in the wells containing the PI3-K inhibitor confirmed the presence of a high frequency of $CD14^+$ cells, denoting the lack of adhesion of the CD14-expressing cells (data not shown). It was also of interest that the addition of various concentrations of soluble or immobilized RANTES, MIP-1α, and MIP-1β did not enhance monocyte adhesion (data not shown), denoting that simple ligation of the chemokine receptors was not sufficient to facilitate adhesion.

It has been previously documented that adhesion of monocytes onto plastic plates is mediated by fibrinogen

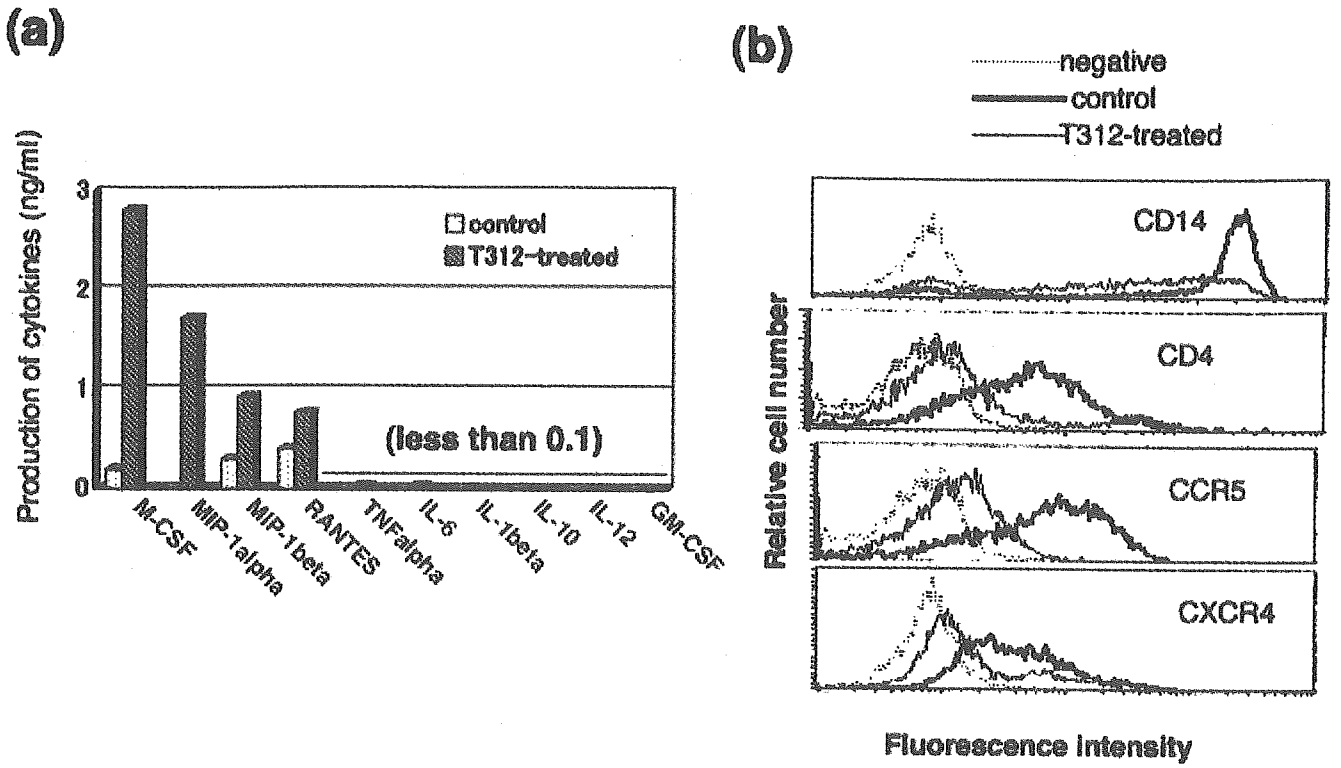

Figure 3. Cytokine profile and phenotypic analysis of purified monocytes following CCR5 cross-linking. (a) CD14 negatively selected monocytes at 2×10^5/ml in RPMI medium in T312 mAb-coated (T312-treated) or control wells (control) were cultured overnight, and cytokines produced in the culture supernatants were assayed by ELISA. Values of <0.1 ng/ml were below the sensitivity of the assay employed. (b) Aliquots of monocytes that were cultured in control wells (thick dark lines) or those cultured in T312 mAb-coated wells (thin dark lines) were analyzed for the expression of CD14, CD4, CCR5, and CXCR4 by routine flow cytometry. The broken lines show background staining of cells with isotype control mAbs.

binding by the β2-integrins Mac-1 (CD11b/CD18) and/or p150/95 (CD11c/CD18) (32, 33). As shown in Figure 2b, the T312 mAb-induced adhesion of monocytes was blocked by anti-CD18 blocking mAb (with specificity for the common chain of β2-integrins), but not anti-CD29 mAb (β1-integrin) or anti-CD11a (another component of the β2-integrin, LFA-1), indicating an involvement of the β2-integrins in the enhanced adhesion of monocytes by T312 mAb-mediated CCR5 cross-linking.

2. Cytokine Profile and Phenotype Analysis of Monocytes Adhered to the T312 mAb-Precoated Wells. In an effort to define the cytokine profile characteristic of the monocyte population, it was reasoned that depletion of nonmonocyte lymphoid cells before analysis would be important. The magnetic bead negative selection technique for $CD14^+$ cells was thus used to deplete such nonmonocyte lymphoid cells, and the subsequent enriched monocytes were then incubated overnight in wells precoated with either T312 or control mAb, and the supernatant fluids were collected. Representative data from three experiments are shown in Figure 3a. As seen, the T312 mAb-stimulated monocytes secreted significant levels of M-CSF, MIP-1α, MIP-1β, and RANTES. The $CD14^+$ monocytes are likely to be the major cell lineage that responded to the T312 mAb stimulation by the production of cytokines, because PBMCs depleted of $CD14^+$ monocytes failed to synthesize detectable levels of the same cytokines. An aliquot of the same supernatants was also screened for levels of GM-CSF, TNF-α, IL-1β, IL-12, or IL-10, but each was found to be below 0.1 ng/ml. A variety of rat and mouse mAbs that had been generated in our laboratory with specificity for HTLV-1, HIV-1, HCV, OX40L, OX40, or IL-2R were also used to precoat the wells and were screened for their ability to induce cytokine synthesis by purified monocytes in parallel with the use of T312 mAb. As expected, only monocytes incubated in the wells precoated with T312 mAb produced M-CSF, MIP-1α, MIP-1β, and RANTES, denoting an element of specificity for the T312 mAb (data not shown).

Phenotypic analysis of monocytes adhered to the T312 mAb-precoated wells consistently showed a marked down-regulation of CD14, CD4, CCR5, and CXCR4 (a representative profile is shown in Figure 3b). Downmodulation of the CD14 on the cell surface was not attributed to the shedding of CD14, since there was no difference in the level of soluble CD14 between the supernatant fluids from the wells precoated with the T312 mAb and those from the control wells, as determined by ELISA (data not shown).

3. CCR5 Cross-Linking Stimulates Monocyte Differentiation into DCs. To test whether the T312 mAb-induced CCR5 cross-linking has the potential to

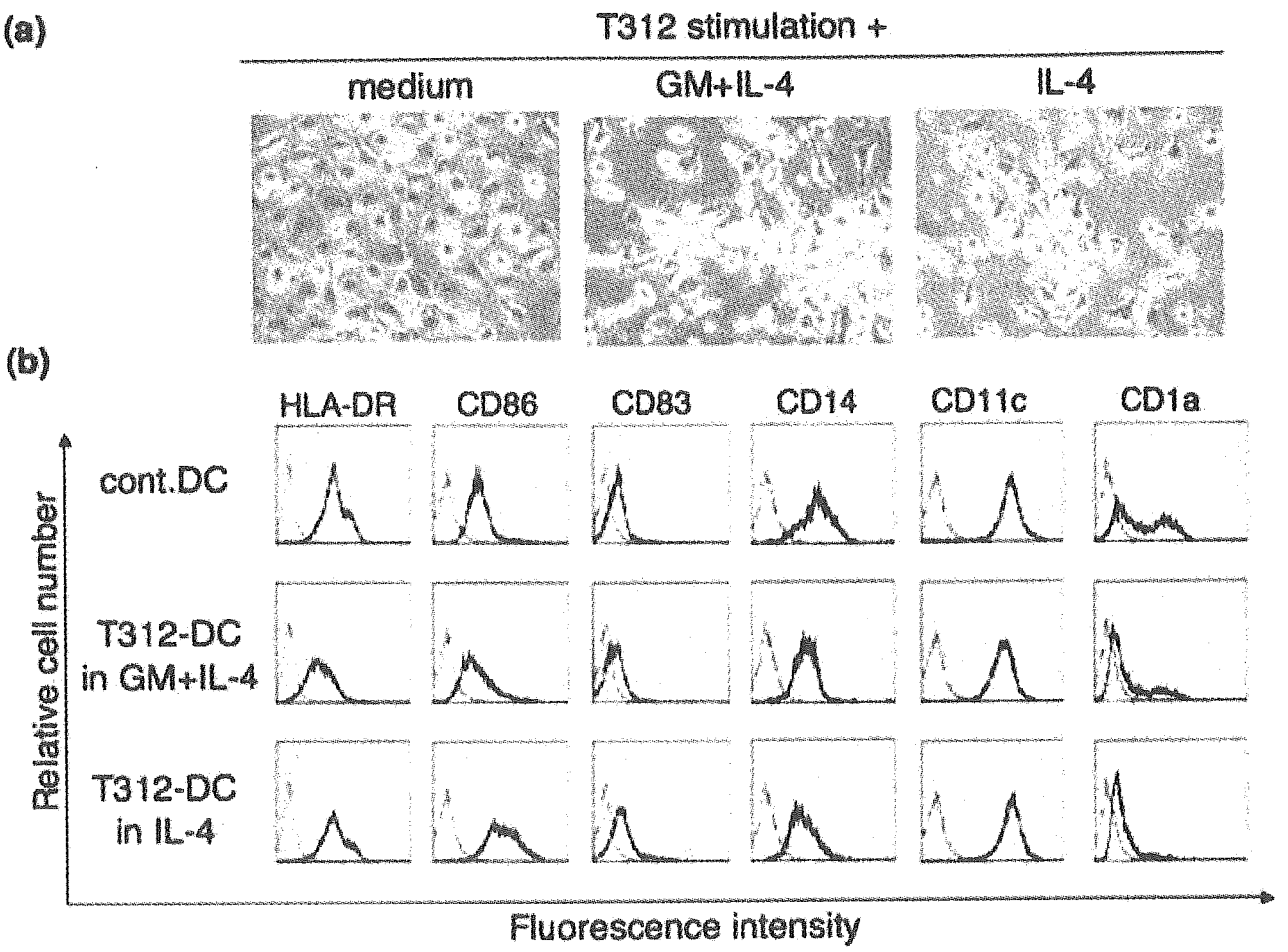

Figure 4. Morphological and flow cytometric analyses of adherent PBMCs following maturation in different culture conditions *in vitro*. (a) PBMCs at 5×10^6/ml in RPMI medium were cultured overnight in wells precoated with T312 mAb. After removal of nonadherent cells, adherent cells were cultured in RPMI medium (medium) or in the presence of 500 ng/ml GM-CSF and 200 ng/ml IL-4 (GM-CSF+IL-4) or 25 ng/ml IL-4 alone (IL-4) for 5 days. Morphology was observed microscopically at ×200. (b) The T312-induced immature DCs were generated from PBMCs adhered to the T312 mAb-coated wells during overnight incubation followed by cultivation in the presence of either GM-CSF and IL-4 (T312-DC in GM+IL-4) or IL-4 alone (T312-DC in IL-4). For comparison, control conventional DCs were generated from 2 hr–adherent PBMCs in control wells followed by cultivation in GM-CSF and IL-4 for 6 days (cont. DC). After maturation for an additional day with IFN-β, aliquots of these cells were subjected to flow cytometric analysis, and the profiles for the expression of HLA-DR, CD86, CD83, CD14, CD11c, and CD1a are shown.

differentiate monocytes into functional DCs, aliquots of PBMCs were first incubated either in the T312 mAb-coated wells overnight or the control mAb-coated wells for 2 hrs (for the generation of conventional DCs), the nonadherent cells were removed, and then the adherent cells were further cultured in the presence or absence of either GM-CSF and IL-4 or IL-4 alone for 5 or 6 days, respectively.

As shown in Figure 4a, the adherent cells incubated in T312-coated wells appeared to have a DC type of morphology, which was confirmed by flow cytometric analysis (see Fig. 4b). Interestingly, the T312 mAb-stimulated monocytes, when cultured in the presence of IL-4, regardless of the presence or absence of GM-CSF, exhibited higher mean density levels of CD86 and lower levels of CD1a than did control conventional DCs that were cultured in media containing both GM-CSF and IL-4. The DCs cultured in the presence of GM-CSF and IL-4 in the T312 mAb-coated wells had a phenotype that was basically similar to that of the ones cultured in IL-4 alone, and these are both representative profiles of immature DCs. Kinetic studies of the differentiation of these T312 mAb-stimulated immature DCs showed that the optimal level of maturation was achieved by cultivation in the presence of IFN-β for an additional day.

We next sought to examine the relative phagocytic activity of monocyte-derived DCs or macrophages that were cultured in various conditions. As seen in Figure 5, macrophages obtained following differentiation of a highly enriched population of CD14+ monocytes in M-CSF–containing media in general gave a higher relative phagocytic index than did DCs generated in media containing GM-CSF and IL-4. In addition, those that were stimulated with T312 mAb and cultured in media containing either GM-CSF and IL-4 or IL-4 alone were less phagocytic

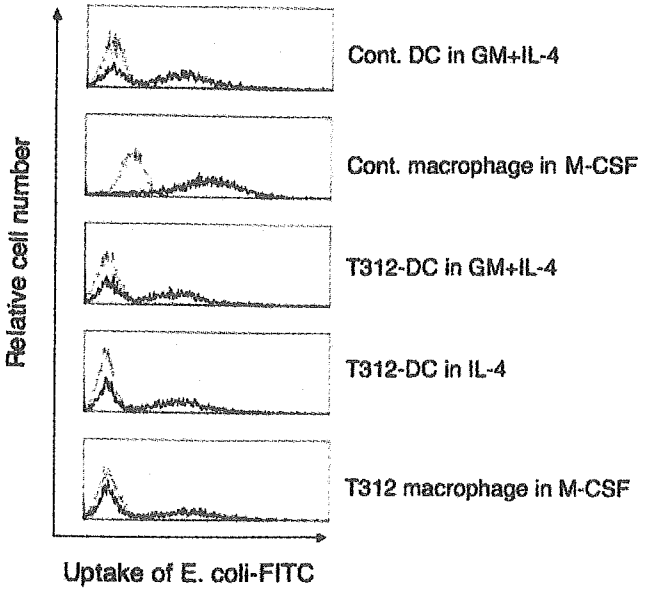

Figure 5. Phagocytic activities of cultured macrophages or immature DCs. Various DCs were generated as described in the legend for Figure 4, and macrophages were generated from 2 hr–adherent PBMCs followed by cultivation in the presence of M-CSF for 6 days. These sample cells in RPMI medium were incubated with a 10-fold excess of FITC-labeled *E. coli* particles for 1 hr at 37°C. After washing, the levels of uptake of FITC-labeled *E. coli* by cells were determined by flow cytometry with gating for macrophages and DCs using standard forward and side scatter.

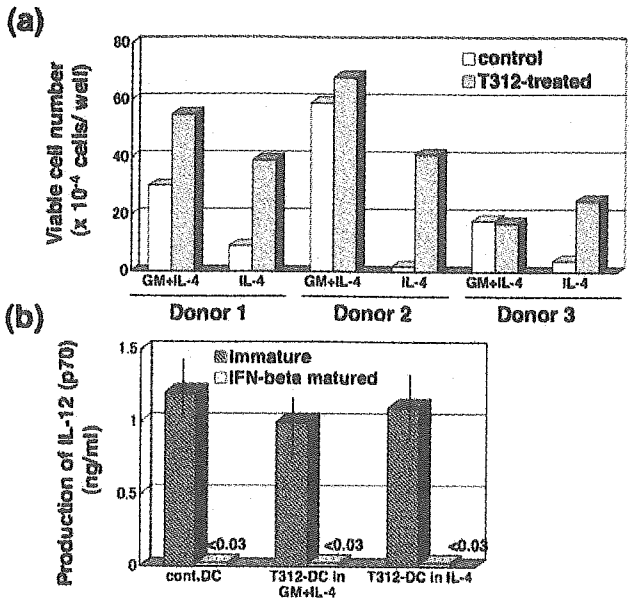

Figure 6. Yields of DCs and IL-12 production. (a) Immature DCs were generated by either incubation of aliquots of PBMCs from three different donors in the control wells (control) or in the T312 mAb-coated wells (T312-treated) and then for 6 or 5 days, respectively, with GM-CSF and IL-4 or IL-4 alone, as described in the legend for Figure 4. Numbers of viable cells that were not stained by eosin-Y were manually counted using a hemocytometer. The means from triplicate determinations are shown. (b) DCs from a donor before (immature) or after IFN-β treatment (mature) were stimulated by 1 μg/ml LPS and 100 ng/ml IFN-γ for 24 hrs. IL-12 p70 levels in the culture supernatants were determined by ELISA.

than the control macrophages generated by M-CSF. Interestingly, the T312 mAb-stimulated monocytes, following incubation with media containing M-CSF alone, gave slightly lower phagocytic values than the normal macrophages cultured in the same media. These data seem to indicate that cross-linking of CCR5 influences monocyte differentiation into DC rather than macrophage, even in the presence of M-CSF.

We further determined the relative levels of viability of the cells that adhered either to the T312-coated wells overnight or to control wells for 2 hrs followed by cultivation in medium alone or media containing either GM-CSF and IL-4 or IL-4 alone for 5 or 6 days, respectively. Figure 6a shows, first of all, that whereas there was variation in the number of viable cells recovered among donors of the PBMCs, the yields of viable cells generated in the T312 mAb-coated or control wells followed by cultivation in GM-CSF and IL-4 were basically similar. In contrast, aliquots of the same cells incubated in T312 mAb-coated or control wells gave different yields following incubation with IL-4 alone. The cells stimulated by T312 mAb gave significantly higher viable yields than those incubated in control wells. The overnight adherent monocytes could differentiate into functional DCs in the presence of GM-CSF and IL-4, but the cell yield was lower than those obtained from the 2-hr adherent cells (data not shown).

Aliquots of these *in vitro*–generated immature DCs were subsequently challenged with LPS and IFN-γ for 48 hrs, and supernatant fluids were assayed for levels of IL-12 p70. Controls consisted of aliquots of the conventional DCs obtained from the same PBMCs in wells coated with control IgG1 instead of T312 mAb. As seen in Figure 6b, there were significant levels of IL-12 synthesized by both these populations of immature DCs, and the importance of the levels appeared quite similar. Furthermore, the IL-12–producing activity of these immature DCs was lost after full maturation by incubation with IFN-β.

4. Function of DCs. In an effort to determine whether the T312 mAb-induced DCs were as competent as conventional DCs, these immature DC populations were matured by cultivation in media containing IFN-β for 1 day and the aliquots dispensed into microtiter wells and standard mixed lymphocyte reaction (MLR) studies performed. The T312 mAb-induced DCs (termed T312/IL-4 or T312/GM-IL-4) and the conventional DCs (termed control/GM-IL-4) were co-cultured with allogeneic naïve $CD4^+$ T cells. Controls consisted of $CD4^+$ T cells cultured alone or DCs cultured alone. The cultures were performed at a DC to T-cell ratio of 1 to 5, and each combination was cultured in triplicate for 7 days and proliferation assessed using BrdU incorporation by the ELISA method. Supernatant fluids from the MLR cultures were also assayed for levels of IFN-γ, IL-4, and IL-10. As shown in Figure 7a, there was no significant difference in the proliferation-inducing activity

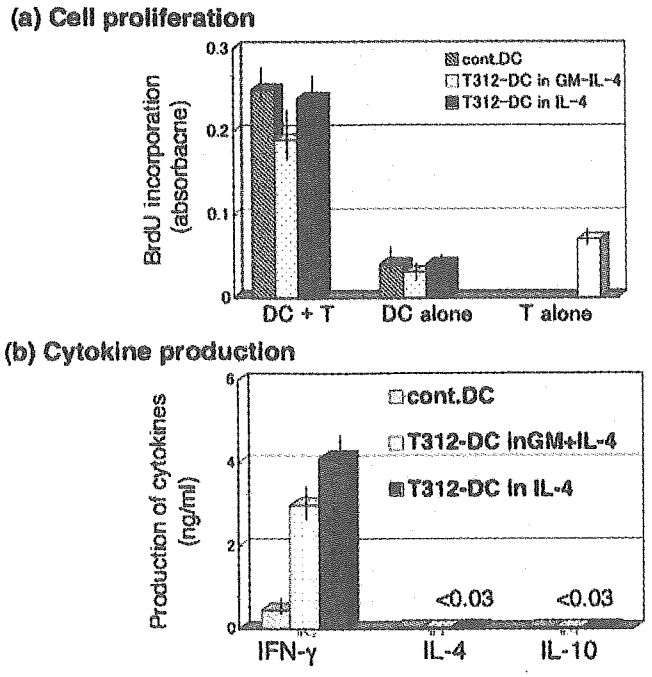

Figure 7. T312 mAb-induced DCs stimulate allogeneic naïve $CD4^+$ T cells to proliferate and produce IFN-γ. Allogeneic naïve $CD4^+$ T cells were co-cultured with IFN-β–matured DCs that had been generated from the adherent PBMCs, as described in the legend for Figure 4 in RPMI medium supplemented with 20 U/ml IL-2 for 7 days. (a) Cell proliferation was determined by BrdU incorporation. Mean values from six wells and standard errors are shown. Controls consisted of culturing either DCs or T cells alone. (b) IFN-γ production in the culture supernatants was determined by ELISA.

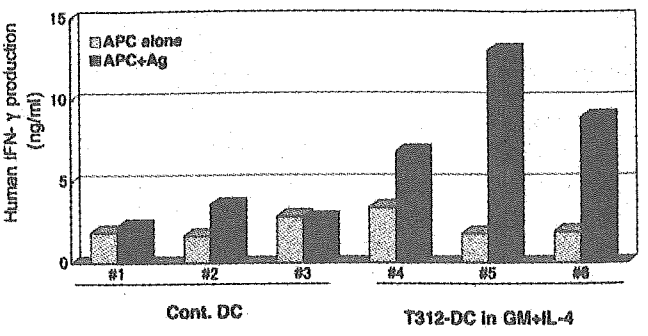

Figure 8. T312 mAb-induced DCs trigger human antigen–specific T-cell responses in hu-PBL-SCID mice. DCs were generated as described in the legend for Figure 4, followed by exposure to antigen (100 μg/ml OVA or KLH) for 24 hrs and by maturation with IFN-β for an additional 24 hrs. These DCs (5×10^5 cells) together with autologous fresh PBMCs (3×10^6 cells) were mixed in 0.1 ml RPMI medium and transplanted into the spleen of SCID mice. Booster immunization was made by injection of the same numbers of antigen-loaded DCs (ip) on Day 7. After 5 days, cells obtained from the spleen and peritoneal cavity of the mice were cultured with autologous APCs (adherent PBMCs during 2-hr incubation in normal wells) in the presence (APC + Ag) or absence (APC alone) of 5 μg/ml OVA for 2 days, and the supernatants were assayed for human IFN-γ by ELISA. Values depicted reflect the mean levels of IFN-γ of triplicate cultures (SD was <10%).

among the three preparations of DCs. However, an obvious difference was seen in the levels of IFN-γ synthesized from the naïve $CD4^+$ T cells (Fig. 7b). The T312 mAb-induced DCs generated in the presence of either GM-CSF and IL-4 or IL-4 alone stimulated higher production of IFN-γ than the control DCs. None of these DCs induced production of IL-4 or IL-10 from the $CD4^+$ T cells by co-culture. The T312 mAb-induced DCs did not produce detectable levels of human IFN-γ, even following stimulation with LPS or CD40L (data not shown), indicating that the allogeneic naïve $CD4^+$ T cells are the likely source of IFN-γ following co-culture and stimulation with DCs. These results indicate that the T312 mAb-induced DCs acquired a relatively higher Th1-polarizing capacity than control conventional DCs.

Furthermore, we tested and compared the ability of these DCs to induce human antigen-specific T- and B-cell immune responses *in vivo*. For this purpose, we used our hu-PBL-SCID mouse model (16). SCID mice were engrafted with normal PBMCs together with antigen (OVA)–pulsed autologous T312 mAb-induced or conventional mature DCs. A booster injection with antigen-pulsed homologous source of mature DCs was performed after 7 days. Immune sera and spleen cells were harvested after 5 days following the booster injection. Figure 8 shows that immunization with the T312 mAb-induced and OVA-pulsed DCs was more efficient in inducing antigen-specific T-cell immune responses in the hu-PBL-SCID mice, as determined and defined by human IFN-γ production by the immune cells *in vitro*, than the conventional DCs pulsed with OVA. IL-4 was not produced from those immune cells (data not shown). Human OVA-specific IgG were also induced by both types of the conventional and T312 mAb-induced DCs up to a titer of 1:400, as determined by ELISA (data not shown). Essentially similar results were obtained when mice were immunized with another antigen, KLH (data not shown). These data indicate that the T312 mAb-induced DCs, in general, appear to be relatively more efficient than conventionally derived DCs in inducing antigen-specific IFN-γ responses *in vivo*.

5. Effect of Cross-Linking by Other mAbs Against Chemokine Receptors. Based on the results from the above studies, additional experiments were carried out to examine the specificity of the ligation of the CCR5 coreceptor by the T312 mAb. Thus, a battery of mAbs against human chemokine receptors expressed by monocytes, including CCR1, CCR2, CCR3, CCR5, CCR8, and CXCR4, were used to precoat microtiter wells, and aliquots of purified monocytes were incubated in such antibody-coated wells. The level of M-CSF synthesized by the cells following overnight incubation was used as an index of monocyte stimulation. As seen in Figure 9 among the anti-human CCR5 mAbs tested, Mab180 (mouse IgG anti-CCR5 N-terminus), but not T227 (rat IgG2a anti-CCR5 N-terminus) or 2D7 (mouse IgG anti-CCR5 ECL-2), was as effective as T312 mAb in the stimulation of monocytes. Among the anti-human CXCR4 mAbs, clone A120 (rat IgG2b anti-CXCR4 ECL1&2) and A80 (rat IgG1 anti-

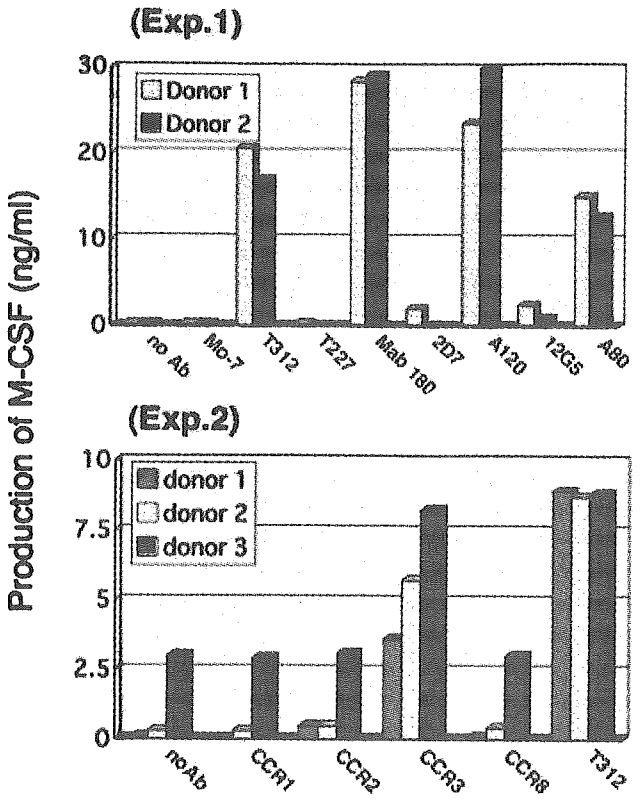

Figure 9. Screening of the other anti-chemokine receptor mAbs that can stimulate monocytes. Purified monocytes at 1×10^5/ml in RPMI medium were cultured in wells precoated with various mAbs overnight, and the culture supernatants were assayed for M-CSF by ELISA. The values depicted represent the mean of triplicate cultures with SD of <10%.

CXCR4 ECL-3) were also capable of stimulating monocytes. Another monocyte-stimulating mAb was the rat IgG2a anti-CCR3 mAb. These mAbs that successfully stimulated monocytes also promoted monocyte adhesion, and A120 anti-CXCR4 mAb in particular was very potent in inducing adhesion and differentiation of monocytes similar to the data derived using the T312 mAb (data not shown). Whether subtle differences exist in the adherent cells enriched by the mAbs that were active in such an assay remains to be determined.

Discussion

In the present study, we present data showing that cross-linking of CCR5 as well as select other chemokine receptors (CXCR4 and CCR3) by mAbs immobilized onto plastic microtiter wells leads to enhanced adhesion of monocytes followed by synthesis of M-CSF and a set of β-chemokines and that incubation of these adherent cells with GM-CSF and IL-4 or IL-4 alone leads to their differentiation along the DC lineage. This functional activity observed following chemokine receptor cross-linking is in contrast to the data obtained with FcR cross-linking (34). This enhanced adherence of monocytes apparently improves the efficacy of adhesion-based monocyte enrichment from fresh PBMCs.

One contributing mechanism that facilitates such tight adhesion may involve the enhanced affinity of the β2-integrins Mac-1 and/or p150/95, which bind to fibrinogen, an extracellular matrix protein, since such adhesion was markedly inhibited in the presence of mAb anti-CD18 (a common chain of the β2-integrin) but not anti-CD11α (a component of another β2-integrin, LFA-1). This view is supported by data obtained by flow cytometric analysis of the T312 mAb-stimulated monocytes, compared to those incubated in control mAb-coated wells. Thus, the T312 mAb-stimulated cells but not the control cells showed a markedly increased density of staining with FITC-fibrinogen, but not with FITC-gelatin or collagen (data not shown). Although sensitization of chemokine receptors by their respective cognate chemokine ligands is known to activate β1- and β2-integrins (5), it is important to note that the addition or precoating of wells with chemokines that bind to CCR5 (i.e., RANTES, MIP-1α, and MIP-1β), respectively, did not induce such enhanced monocyte adhesion *in vitro* in the present study (data not shown). Thus, it is likely that antibody-mediated cross-linking of chemokine receptors initiates an enhanced degree of activation of monocytes, probably through an extraordinary degree of polarization of the receptors onto the plates. This is supported by the observations made by Lee *et al.* (35) that the mode of monocyte activation by cross-linking of chemokine receptors by gp120 of HIV-1 particles was stronger than that induced by a simple interaction between CCR5 and CXCR4 with their respective chemokines. The inhibition of the T312 mAb-induced monocyte adhesion by the PI3-K-specific inhibitor LY294.002 indicates that the T312 mAb-mediated CCR5 cross-linking also stimulates the G-protein signal cascade, as documented previously for gp120 of HIV-1 (35) and chemokines (36). Since PI3-K activation by chemokines also induces polarization of adhesion molecules and facilitates migration (5, 37), it is likely that it is either the mere strength of the signal that is induced by cross-linking of CCR5 by T312 mAb or the potential pulling together of additional, as-yet-unknown proteins that distinguishes between enhanced adhesion and mere signaling.

It is worth noting that the tight adhesion was not induced by another rat IgG anti-CCR5 mAb, termed clone T227. The difference between anti-CCR5 clone T312 and T227 is that the T227 mAb recognizes a region located within the N-terminus of the CCR5 molecule that has been further localized to a peptide spanning the CCR5 N-terminus amino acids 1–20 but not 2–21, whereas the clone T312 mAb recognizes both of the peptides, with an affinity similar to the clone T227 mAb (Tanaka *et al.*, unpublished data). These two mAbs compete with each other in binding to CCR5. Thus, these results indicate that activation of monocyte by CCR5 cross-linking is epitope-dependent rather than antibody affinity-dependent. This view is further supported by the observation that the use of yet another

immobilized CCR5-specific clone, ECL-2 mAb, did not lead to enhanced adhesion of monocytes, indicating a requirement for epitope specificity to facilitate adhesion. Similarly, with regard to CXCR4, the clones A145 mAb (anti–N-terminus) and 12G5 (anti-ECL1&2) did not induce significant monocyte adhesion, in contrast to A120 mAb (anti-ECL1&2) and A80 mAb (anti–ECL-3). The clone A120 mAb blocks the binding of SDF-1 (the natural ligand for CXCR4) and inhibits infection by the CXCR4-tropic HIV-1 strains, whereas the clone A80 mAb does not block SDF-1 binding but stimulates homologous T-cell aggregation and thus enhances infection of the CXCR4 and CCR5-tropic HIV-1 strains (25). However, it is still unclear which regions (epitopes) of each chemokine receptor are the hot spots for the induction of strong activation signals on monocytes, and this topic thus requires further study.

Along with the enhanced adhesion facilitated by cross-linking of the chemokine receptor, such cross-linking also induced downmodulation of cell surface expression of CD14, CD4, CCR5, and CXCR4 and cytokine production by monocytes. It is of interest that similar effects on monocytes have been induced by prokineticin 1 (PK1)/endocrine gland-derived vascular endothelial growth factor (EG-VEGF), and its G protein-coupled receptors (PKR1 and PKR2) (38). Downregulation of CD14 was reported to be induced by IL-4 or IL-13 at the transcriptional level (39) or by shedding, which was induced by antibody-mediated cross-linking of CD14 or stimulation by LPS and IFN-γ (40). However, these are not the likely mechanisms in studies reported herein, since there was little if any production of IL-4 and IL-13 and no detectable levels of soluble CD14 in the culture supernatants. It has been shown that downmodulation of cell surface expression of CD14, CD4, and CXCR4, but not CCR5 on monocytes, is induced by PKC activation by PMA (41, 42) and that CCR5 downmodulation is induced by CCR5-binding chemokines at only high concentrations as a result of CCR5 internalization (43). Whether these pathways are activated by cross-linking of the chemokine receptors is currently not known. It has also been shown that there is a molecular association between CD4 and the chemokine receptors or among the various chemokine receptors (44, 45). Thus, it can be speculated that CCR5 or CXCR4 cross-linking may induce homo- or hetero-oligomerization of the cell surface CD14, CD4, CXCR4, and/or CCR5, and is then internalized.

In the early studies on monocyte adhesion (5) it was shown that adherence onto plastic plates stimulates monocytes to activate M-CSF, IL-1β, or TNF-α gene expression and that LPS stimulation further enhances the synthesis of these cytokines. Similarly, activation of monocytes via the PK1 pathway following adhesion requires additional stimulation by LPS to promote the production of IL-12 p70 and TNF-α (46). Thus, it is clear that the mechanisms for cytokine production in the studies described herein likely involve distinct pathways other than those discussed above. In addition, the addition of soluble chemokines or the use of immobilized chemokines with specificity for CCR5 and CXCR4 did not induce cytokine production in the present conditions (data not shown). Differences in the precise pathways that are triggered in the studies reported herein are a subject of current study.

The observation that not only CCR5 but also CXCR4 and CCR3 cross-linking triggered production of M-CSF by monocytes and induced differentiation in the absence of exogenously added M-CSF or GM-CSF was unexpected. For differentiation of monocytes into macrophages *in vitro* in the absence of these cytokines, extracellular matrix proteins are known to have profound influence (47). It has been previously reported that human monocytes differentiated into CD14-low macrophages in a fibronectin-containing medium without the addition of exogenous cytokines (48). Thus, bovine fibronectin in our RPMI medium may have some additive effects on chemokine receptor–stimulated monocyte differentiation, although the use of serum-free medium for monocyte cultivation in T312 mAb-coated wells did not influence the present results (data not shown). Although cross-linking of CCR5, CXCR4, or CCR3 resulted in M-CSF production from monocytes, anti-M-CSF– or GM-CSF–neutralizing mAbs did not block monocyte differentiation into macrophages (data not shown). Thus, we assume that chemokine receptor cross-linking may bypass the requirement of M-CSF stimulation. Since the ligation of M-CSF receptor (CD115) stimulates PI3-K (49, 50), the PI3-K activation as a result of the chemokine receptor cross-linking may be responsible for the *de novo* monocyte differentiation into macrophages. The mechanisms by which cross-linking of chemokine receptors on monocytes induced the differentiation of these cells into DCs without the addition of exogenous GM-CSF in the presence of IL-4 are also under current study. The cross-linking may function as survival and differentiation factor for the generation of DCs from monocytes, because monocytes in the absence of chemokine receptor cross-linking failed to survive when cultured in media containing IL-4 alone.

The primary objective of the present study was to find an alternate, more-efficient and practical method for the *in vitro* generation of functional DCs with potent Th1-inducing capacity *in vivo*. Various cytokine cocktails have been applied for generation of functional DCs, including combinations of IL-3 and IFN-β, Flt3L and IL-4, CD40L alone, or GM-CSF, IL-4, and the proinflammatory cytokines GM-CSF and Type I IFN (51–56). In addition, it has been reported that the methods of monocyte isolation, such as adherence or $CD14^+$ enrichment by MACS (which results in CD14 cross-linking), influence cytokine production from generated DCs (i.e., adherent monocyte-derived DCs were more potent in producing IL-12, IL-10, and TNF-α and in stimulating Tc1 than those from CD14 positively selected monocytes) (24). Because the DCs generated in the studies reported herein by CCR5 (or CXCR4 or CCR3) cross-linking in the presence of either GM-CSF and IL-4 or IL-4

alone were relatively more potent than conventional DCs in stimulating IFN-γ production from allogeneic naïve $CD4^+$ T cells *in vitro* and OVA- or KLH-specific T cells *in vivo*, it is indicated that in studies that require Th1-polarizing DCs, the cross-linking of CCR5, CXCR4, or CCR3 on monocytes should be considered. The higher density of expression of CD86 on the chemokine receptor cross-linked DCs may have some influence for Th1-inducing capacity, although the mechanism at present still remains unknown.

Based on the results of the present study, we suggest that the use of cross-linking of CCR5, CXCR4, or other chemokine receptors for the generation of functional DCs *ex vivo* provides an alternate and simple tool that will facilitate the therapeutic use of DCs. Thus, studies of DC-based immunotherapy in patients with HIV-1 infection that have been reasoned to require induction of maintenance of Th1 type of antiviral immune response could benefit from such an approach. In addition, cross-linking of the chemokine receptors could also facilitate limited entry of HIV-1 into such cells because of downmodulation of the HIV-1 receptors. Such an approach has already been initiated, and preliminary studies have shown that inactivated HIV-1–pulsed DCs generated from CCR5– and CXCR4–cross-linked monocytes could trigger highly potent human anti–HIV-1 T-cell responses using our hu-PBL-SCID mouse model. These studies are currently in progress.

We thank the NIH AIDS Research and Reference Reagent Program for supplying IL-2.

1. van Furth R, Cohn ZA. The origin and kinetics of mononuclear phagocytes. J Exp Med 128:415–435, 1968.
2. Warren MK, Vogel SN. Bone marrow-derived macrophages: development and regulation of differentiation markers by colony-stimulating factor and interferons. J Immunol 134:982–989, 1985.
3. Steinman RM. The dendritic cell system and its role in immunogenicity. Annu Rev Immunol 9:271–296, 1991.
4. Zhou LJ, Tedder TF. CD14+ blood monocytes can differentiate into functionally mature CD83+ dendritic cells. Proc Natl Acad Sci U S A 93:2588–2592, 1996.
5. Imhof BA, Aurrand-Lions M. Adhesion mechanisms regulating the migration of monocytes. Nat Rev Immunol 4:432–444, 2004.
6. Mellado M, Rodriguez-Frade JM, Manes S, Martinez AC. Chemokine signaling and functional responses: the role of receptor dimerization and TK pathway activation. Annu Rev Immunol 19:397–421, 2001.
7. Pulendran B, Palucka K, Banchereau J. Sensing pathogens and tuning immune responses. Science 293:253–256, 2001.
8. Donaghy H, Pozniak A, Gazzard B, Qazi N, Gilmour J, Gotch F, Patterson S. Loss of blood CD11c(+) myeloid and CD11c(–) plasmacytoid dendritic cells in patients with HIV-1 infection correlates with HIV-1 RNA virus load. Blood 98:2574–2576, 2001.
9. Soumelis V, Scott I, Gheyas F, Bouhour D, Cozon G, Cotte L, Huang L, Levy JA, Liu YJ. Depletion of circulating natural type 1 interferon-producing cells in HIV-infected AIDS patients. Blood 98:906–912, 2001.
10. Urban BC, Ferguson DJ, Pain A, Willcox N, Plebanski M, Austyn JM, Roberts DJ. Plasmodium falciparum-infected erythrocytes modulate the maturation of dendritic cells. Nature 400:73–77, 1999.
11. Fugier-Vivier I, Servet-Delprat C, Rivailler P, Rissoan MC, Liu YJ, Rabourdin-Combe C. Measles virus suppresses cell-mediated immunity by interfering with the survival and functions of dendritic and T cells. J Exp Med 186:813–823, 1997.
12. Fong L, Engleman EG. Dendritic cells in cancer immunotherapy. Annu Rev Immunol 18:245–273, 2000.
13. Lu W, Arraes LC, Ferreira WT, Andrieu JM. Therapeutic dendritic-cell vaccine for chronic HIV-1 infection. Nat Med 10:1359–1365, 2004.
14. Garcia F, Lejeune M, Climent N, Gil C, Alcami J, Morente V, Alos L, Ruiz A, Setoain J, Fumero E, Castro P, Lopez A, Cruceta A, Piera C, Florence E, Pereira A, Libois A, Gonzalez N, Guila M, Caballero M, Lomena F, Joseph J, Miro JM, Pumarola T, Plana M, Gatell JM, Gallart T. Therapeutic immunization with dendritic cells loaded with heat-inactivated autologous HIV-1 in patients with chronic HIV-1 infection. J Infect Dis 191:1680–1685, 2005.
15. Lu W, Wu X, Lu Y, Guo W, Andrieu JM. Therapeutic dendritic-cell vaccine for simian AIDS. Nat Med 9:27–32, 2003.
16. Yosida A, Tanaka R, Murakami T, Takahashi Y, Koyanagi Y, Nakamura M, Ito M, Yamamoto N, Tanaka Y. Induction of protective immune responses against R5 human immunodeficiency virus type 1 (HIV-1) infection in hu-PBL-SCID mice by intrasplenic immunization with HIV-1–pulsed dendritic cells: possible involvement of a novel factor of human $CD4^+$ T-cell origin. J Virol 77:8719–8728, 2003.
17. Lapenta C, Santini SM, Logozzi M, Spada M, Andreotti M, Di Pucchio T, Parlato S, Belardelli F. Potent immune response against HIV-1 and protection from virus challenge in hu-PBL-SCID mice immunized with inactivated virus-pulsed dendritic cells generated in the presence of IFN-alpha. J Exp Med 198:361–367, 2003.
18. Wu L, Dakic A. Development of dendritic cell system. Cell Mol Immunol 1:112–118, 2004.
19. Banchereau J, Steinman RM. Dendritic cells and the control of immunity. Nature 392:245–252, 1998.
20. D'Amico A, Wu L. The early progenitors of mouse dendritic cells and plasmacytoid predendritic cells are within the bone marrow hemopoietic precursors expressing Flt3. J Exp Med 198:293–303, 2003.
21. Romani N, Reider D, Heuer M, Ebner S, Kampgen E, Eibl B, Niederwieser D, Schuler G. Generation of mature dendritic cells from human blood. An improved method with special regard to clinical applicability. J Immunol Methods 196:137–151, 1996.
22. Sallusto F, Lanzavecchia A. Efficient presentation of soluble antigen by cultured human dendritic cells is maintained by granulocyte/macrophage colony-stimulating factor plus interleukin 4 and downregulated by tumor necrosis factor alpha. J Exp Med 179:1109–1118, 1994.
23. Tuyaerts S, Noppe SM, Corthals J, Breckpot K, Heirman C, De Greef C, Van Riet I, Thielemans K. Generation of large numbers of dendritic cells in a closed system using Cell Factories. J Immunol Methods 264: 135–151, 2002.
24. Elkord E, Williams PE, Kynaston H, Rowbottom AW. Human monocyte isolation methods influence cytokine production from in vitro generated dendritic cells. Immunology 114:204–212, 2005.
25. Tanaka R, Yoshida A, Murakami T, Baba E, Lichtenfeld J, Omori T, Kimura T, Tsurutani N, Fujii N, Wang ZX, Peiper SC, Yamamoto N, Tanaka Y. Unique monoclonal antibody recognizing the third extracellular loop of CXCR4 induces lymphocyte agglutination and enhances human immunodeficiency virus type 1-mediated syncytium formation and productive infection. J Virol 75:11534–11543, 2001.
26. Grage-Griebenow E, Flad HD, Ernst M. Heterogeneity of human peripheral blood monocyte subsets. J Leukoc Biol 69:11–20, 2001.
27. Ohteki T, Fukao T, Suzue K, Maki C, Ito M, Nakamura M, Koyasu S. Interleukin 12-dependent interferon gamma production by CD8alpha+ lymphoid dendritic cells. J Exp Med 189:1981–1986, 1999.
28. Tanaka Y, Zeng L, Shiraki H, Shida H, Tozawa H. Identification of a neutralization epitope on the envelope gp46 antigen of human T cell leukemia virus type I and induction of neutralizing antibody by peptide immunization. J Immunol 147:354–360, 1991.

29. Inudoh M, Kato N, Tanaka Y. New monoclonal antibodies against a recombinant second envelope protein of hepatitis C virus. Microbiol Immunol 42:875–877, 1998.
30. Tozawa H, Andoh S, Takayama Y, Tanaka Y, Lee B, Nakamura H, Hayami M, Hinuma Y. Species-dependent antigenicity of the 34-kDa glycoprotein found on the membrane of various primate lymphocytes transformed by human T-cell leukemia virus type-I (HTLV-I) and simian T-cell leukemia virus (STLV-I). Int J Cancer 41:231–238, 1988.
31. Magaud JP, Sargent I, Mason DY. Detection of human white cell proliferative responses by immunoenzymatic measurement of bromodeoxyuridine uptake. J Immunol Methods 106:95–100, 1988.
32. Patarroyo M, Prieto J, Beatty PG, Clark EA, Gahmberg CG. Adhesion-mediating molecules of human monocytes. Cell Immunol 113:278–289, 1988.
33. Davis GE. The Mac-1 and p150,95 beta 2 integrins bind denatured proteins to mediate leukocyte cell-substrate adhesion. Exp Cell Res 200:242–252, 1992.
34. MacIntyre EA, Roberts PJ, Jones M, Van der Schoot CE, Favalaro EJ, Tidman N, Linch DC. Activation of human monocytes occurs on cross-linking monocytic antigens to an Fc receptor. J Immunol 142:2377–2383, 1989.
35. Lee C, Liu QH, Tomkowicz B, Yi Y, Freedman BD, Collman RG. Macrophage activation through CCR5- and CXCR4-mediated gp120-elicited signaling pathways. J Leukoc Biol 74:676–682, 2003.
36. Mellado M, Rodriguez-Frade JM, Manes S, Martinez AC. Chemokine signaling and functional responses: the role of receptor dimerization and TK pathway activation. Annu Rev Immunol 19:397–421, 2001.
37. Vicente-Manzanares M, Rey M, Jones DR, Sancho D, Mellado M, Rodriguez-Frade JM, del Pozo MA, Yanez-Mo M, de Ana AM, Martinez AC, Merida I, Sanchez-Madrid F. Involvement of phosphatidylinositol 3-kinase in stromal cell-derived factor-1 alpha-induced lymphocyte polarization and chemotaxis. J Immunol 163:4001–4012, 1999.
38. Dorsch M, Qiu Y, Soler D, Frank N, Duong T, Goodearl A, O'Neil S, Lora J, Fraser CC. PK1/EG-VEGF induces monocyte differentiation and activation. J Leukoc Biol 78:426–434, 2005.
39. Lauener RP, Goyert SM, Geha RS, Vercelli D. Interleukin 4 down-regulates the expression of CD14 in normal human monocytes. Eur J Immunol 20:2375–2381, 1990.
40. Bazil V, Strominger JL. Shedding as a mechanism of down-modulation of CD14 on stimulated human monocytes. J Immunol 147:1567–1574, 1991.
41. Signoret N, Oldridge J, Pelchen-Matthews A, Klasse PJ, Tran T, Brass LF, Rosenkilde MM, Schwartz TW, Holmes W, Dallas W, Luther MA, Wells TN, Hoxie JA, Marsh M. Phorbol esters and SDF-1 induce rapid endocytosis and down modulation of the chemokine receptor CXCR4. J Cell Biol 139:651–664, 1997.
42. Signoret N, Rosenkilde MM, Klasse PJ, Schwartz TW, Malim MH, Hoxie JA, Marsh M. Differential regulation of CXCR4 and CCR5 endocytosis. J Cell Sci 111:2819–2830, 1998.
43. Xiao X, Wu L, Stantchev TS, Feng YR, Ugolini S, Chen H, Shen Z, Riley JL, Broder CC, Sattentau QJ, Dimitrov DS. Constitutive cell surface association between CD4 and CCR5. Proc Natl Acad Sci U S A 96:7496–7501, 1999.
44. Rodriguez-Frade JM, del Real G, Serrano A, Hernanz-Falcon P, Soriano SF, Vila-Coro AJ, de Ana AM, Lucas P, Prieto I, Martinez-A C, Mellado M. Blocking HIV-1 infection via CCR5 and CXCR4 receptors by acting in trans on the CCR2 chemokine receptor. EMBO J 23:66–76, 2004.
45. Ugolini S, Moulard M, Mondor I, Barois N, Demandolx D, Hoxie J, Brelot A, Alizon M, Davoust J, Sattentau QJ. HIV-1 gp120 induces an association between CD4 and the chemokine receptor CXCR4. J Immunol 159:3000–3008, 1997.
46. Cosentino G, Soprana E, Thienes CP, Siccardi AG, Viale G, Vercelli D. IL-13 down-regulates CD14 expression and TNF-alpha secretion in normal human monocytes. J Immunol 155:3145–3151, 1995.
47. Juliano RL, Haskill S. Signal transduction from the extracellular matrix. J Cell Biol 120:577–585, 1993.
48. Jacob SS, Shastry P, Sudhakaran PR. Monocyte-macrophage differentiation in vitro: modulation by extracellular matrix protein substratum. Mol Cell Biochem 233:9–17, 2002.
49. Hamilton JA. CSF-1 signal transduction. J Leukoc Biol 62:145–155, 1997.
50. Varticovski L, Druker B, Morrison D, Cantley L, Roberts T. The colony stimulating factor-1 receptor associates with and activates phosphatidylinositol-3 kinase. Nature 342:699–702, 1989.
51. Carbonneil C, Aouba A, Burgard M, Cardinaud S, Rouzioux C, Langlade-Demoyen P, Weiss L. Dendritic cells generated in the presence of granulocyte-macrophage colony-stimulating factor and IFN-alpha are potent inducers of HIV-specific CD8 T cells. AIDS 17: 1731–1740, 2003.
52. Mohty M, Vialle-Castellano A, Nunes JA, Isnardon D, Olive D, Gaugler B. IFN-alpha skews monocyte differentiation into Toll-like receptor 7-expressing dendritic cells with potent functional activities. J Immunol 171:3385–3393, 2003.
53. Nagai T, Devergne O, Mueller TF, Perkins DL, van Seventer JM, van Seventer GA. Timing of IFN-beta exposure during human dendritic cell maturation and naive Th cell stimulation has contrasting effects on Th1 subset generation: a role for IFN-beta-mediated regulation of IL-12 family cytokines and IL-18 in naive Th cell differentiation. J Immunol 171:5233–5243, 2003.
54. Dauer M, Obermaier B, Herten J, Haerle C, Pohl K, Rothenfusser S, Schnurr M, Endres S, Eigler A. Mature dendritic cells derived from human monocytes within 48 hours: a novel strategy for dendritic cell differentiation from blood precursors. J Immunol 170:4069–4076, 2003.
55. Brossart P, Grunebach F, Stuhler G, Reichardt VL, Mohle R, Kanz L, Brugger W. Generation of functional human dendritic cells from adherent peripheral blood monocytes by CD40 ligation in the absence of granulocyte-macrophage colony-stimulating factor. Blood 92:4238–4247, 1998.
56. Buelens C, Bartholome EJ, Amraoui Z, Boutriaux M, Salmon I, Thielemans K, Willems F, Goldman M. Interleukin-3 and interferon beta cooperate to induce differentiation of monocytes into dendritic cells with potent helper T-cell stimulatory properties. Blood 99:993–998, 2002.

Induction of Positive Cellular and Humoral Immune Responses by a Prime-Boost Vaccine Encoded with Simian Immunodeficiency Virus *gag/pol*[1]

Kenji Someya,* Yasushi Ami,† Tadashi Nakasone,* Yasuyuki Izumi,* Kazuhiro Matsuo,* Shigeo Horibata,* Ke-Qin Xin,‡ Hiroshi Yamamoto,§ Kenji Okuda,‡ Naoki Yamamoto,* and Mitsuo Honda[2]*

It is believed likely that immune responses are responsible for controlling viral load and infection. In this study, when macaques were primed with plasmid DNA encoding SIV *gag* and *pol* genes (SIV*gag/pol* DNA) and then boosted with replication-deficient vaccinia virus DIs recombinant expressing the same genes (rDIsSIV*gag/pol*), this prime-boost regimen generated higher levels of Gag-specific CD4$^+$ and CD8$^+$ T cell responses than did either SIV*gag/pol* DNA or rDIsSIV*gag/pol* alone. When the macaques were i.v. challenged with pathogenic simian/HIV, the prime-boost group maintained high CD4$^+$ T cell counts and reduced plasma viral loads up to 30 wk after viral challenge, whereas the rDIsSIV*gag/pol* group showed only a partial attenuation of the viral infection, and the group immunized with SIV*gag/pol* DNA alone showed none at all. The protection levels were better correlated with the levels of virus-specific T cell responses than the levels of neutralization Ab responses. These results demonstrate that a vaccine regimen that primes with DNA and then boosts with a replication-defective vaccinia virus DIs generates anti-SIV immunity, suggesting that it will be a promising vaccine regimen for HIV-1 vaccine development. *The Journal of Immunology,* **2006, 176: 1784–1795.**

The primary goals of any prophylactic HIV vaccine are to induce HIV-specific immune responses capable of preventing the malfunctioning of immune systems and to limit viral transmission due to replication. Clinical studies have demonstrated that CTL immune responses are associated with the reduction of plasma viral load (1, 2) and can control disease progression (3, 4). Replication of pathogenic SIV in vivo has also been shown to be controlled in the macaque model by CD8$^+$ T cell responses (5). Because amino acid sequences of Gag and Pol of HIV-1 proteins are relatively conserved, cross-clade and broad CTL responses targeting those proteins have been observed in both HIV-infected and HIV-exposed individuals, even if the latter group had not become infected (6–8). Thus, one recent focus of HIV vaccine research has been to elicit more protective antiviral immune responses by enhancing the expression levels of HIV-1 Ags of Gag and Pol using a safe vaccine vector.

Recently, several prime-boost regimens consisting of a DNA prime and a recombinant poxvirus boost targeting the immunodeficiency virus have been reported to generate higher levels of HIV-specific T cell immune responses than regimens relying on DNA or recombinant poxvirus vaccine alone (9, 10). In efficacy trials of such heterologous prime-boost vaccines, an SIV Ag encoding DNA prime and a boost of recombinant modified vaccinia virus Ankara (MVA)[3] elicited effective anti-SIV immunity and controlled infection of the nonpathogenic simian-HIV (SHIV) strain as well as of the pathogenic strain SHIV-89.6P in macaques (11–13) by effectively inducing CD8$^+$ CTL immunities. Various poxvirus vectors, i.e., an avipox virus, a canarypox virus, a fowlpox virus, a substrain of vaccinia Copenhagen (NYVAC), and MVA, have been evaluated for their usefulness, either alone or in combination with other vaccine modalities (14–18). To be useful, these vaccine vectors must, of course, be safe. The currently widely used MVA, which was developed toward the end of the campaign to eradicate small pox, has been effectively and safely used in >100,000 people as a small pox vaccine (19). MVA-based recombinant vector has also been reported to be safe in animals (20, 21). Lately, we have developed a replication-defective vaccinia virus DIs strain as a vaccine vector (22, 23). The DIs strain, generated by a 1-day-old egg passage of the DIE strain (24), has been proven safe (25, 26). We also suggested that a new prime-boost vaccine regimen consisting of SIV*gag/pol* DNA and rDIsSIV*gag/pol* might be useful for the development of an HIV-1 candidate vaccine that could induce strong cellular protective responses in mice (23). Lately, similar DNA/MVA vaccine combinations support the idea that the vaccine induced strong Ag-specific T and B cell responses (27). The prime-boost-vaccinated mice generated higher levels of both Gag-specific CD4$^+$ and CD8$^+$ T cell immune responses than those vaccinated with either DNA or rDIs alone. When such mice were challenged with SIV *gag/pol* expressing

*AIDS Research Center, National Institute of Infectious Diseases, Tokyo, Japan; †Division of Experimental Animal Research, National Institute of Infectious Diseases, Tokyo, Japan; ‡Department of Bacteriology, Yokohama City University, School of Medicine, Yokohama, Japan; and §Laboratory Animal Research Center, Toyama Medical and Pharmaceutical University, Toyama, Japan

Received for publication June 28, 2005. Accepted for publication November 4, 2005.

The costs of publication of this article were defrayed in part by the payment of page charges. This article must therefore be hereby marked *advertisement* in accordance with 18 U.S.C. Section 1734 solely to indicate this fact.

[1] This work was supported by the Panel on AIDS of the U.S.-Japan Cooperative Medical Science Program; the Human Science Foundation, Japan; the Japanese Ministry of Health, Labor, and Welfare; and the AIDS Vaccine Project in conjunction with the Japan Science and Technology Corporation.

[2] Address correspondence and reprint requests to Dr. Mitsuo Honda, AIDS Research Center, National Institute of Infectious Diseases, 1-23-1 Toyama, Shinjuku-ku, Tokyo 162-8640, Japan. E-mail address: mhonda@nih.go.jp

[3] Abbreviations used in this paper: MVA, modified vaccinia virus Ankara; rDIsSIV*gag/pol*, recombinant DIs expressing SIV*gag* and *pol*; SFC, spot-forming cell; SHIV, simian-human immunodeficiency virus; SIV*gag/pol* DNA, plasmid DNA encoding SIV *gag* and *pol* genes; $TCID_{50}$, 50% tissue culture infectious doses.

0022-1767/06/$02.00

wild-type recombinant vaccinia virus, viral replication in the ovaries was controlled even in the absence of anti-DIs immunity. These results suggest that the new vaccine regimen, consisting of a DNA prime and a vaccinia virus DIs boost, safely and effectively elicits anti-immunodeficiency viral immunity.

In this study, we evaluated the vaccine efficacy of the prime-boost DNA/DIs vaccine encoding the *gag/pol* gene against a challenge with a highly pathogenic SHIV using 19 macaques. We hypothesize that the efficacy is mediated not only by the effect of virus-specific cellular immunity, but also by the effect of neutralization Ab responses against the challenged virus.

Materials and Methods

Animals

Nineteen female adult cynomolgus macaques (*Macaca fascicularis*) were purchased from Japan SLC. The macaques were fed and cared for in accordance with the standard operating procedure approved by the Ministry of Education, Culture, Sports, Science, and Technology of Japan. The study was performed in the P3 facility under guidelines established by the laboratory biosafety manual of the World Health Organization (28).

Preparation of vaccine Ags and challenge virus

Plasmid DNA encoding SIV *gag* and *pol* genes (SIV*gag/pol* DNA) and recombinant DIs expressing the same genes (rDIsSIV*gag/pol*) were prepared as previously described (22, 23, 29). pcDNA3.1$^-$ and rDIsLacZ were used as controls of plasmid and recombinant viral Ags, respectively. After being immunized according to the protocol, animals were challenged with SHIV-C2/1 (30–32), which was a SHIV-89.6 variant isolated at the peak of initial plasma viremia from an infected cynomolgus macaque (31). The original SHIV strain was provided by Dr. Y. Lu (Harvard AIDS Institute, Cambridge, MA) (33, 34).

Enumeration of T PBL

Fifty microliters of whole heparinized blood samples were stained with anti-human CD3 (clone HIT3a; BD Pharmingen), anti-human CD4 (clone SK3; BD Biosciences), and anti-human CD8 (clone SK1; BD Biosciences) for 15 min at 4°C. Blood samples were treated with FACS lysing solution for 15 min at 4°C, and then 50 μl of Flow Count (Beckman Coulter) was added. A FACSCalibur flow cytometer (BD Biosciences) was used to acquire 5000 CD3-positive, lymphocyte-gated events.

Intracellular IFN-γ cytokine staining

Approximately 10^6 of fresh PBMC were incubated with 0.2 μM pooled SIV Gag peptides spanning the full length of the Gag protein (AIDS Research and Reference Program, National Institutes of Health) together with 1 μg of anti-human CD28 (clone KOLT-2; Nichirei) and 1 μg of anti-human CD49d (clone 9F10; BD Pharmingen) in an appropriate volume of RPMI 1640 supplemented with 10% FBS and antibiotics for 16 h at 37°C. Then brefeldin A (Sigma-Aldrich) was added at 10 μg/ml, and the cells were incubated for an additional 4 h. After incubation, the cells were washed, stained with anti-human CD3 (clone HIT3a; BD Pharmingen) and anti-human CD8 (clone SK1; BD Biosciences) or anti-human CD4 (clone SK3; BD Biosciences) for 15 min. The cells were washed and then treated sequentially with FACS-lysing solution (BD Biosciences) and permeablizing solution (BD Biosciences) for 10 min. The cells were stained with anti-human IFN-γ-FITC (clone 45.15; Immuno Tech) for 30 min and fixed with 2% paraformaldehyde solution. A FACSCalibur flow cytometer (BD Biosciences) was used to acquire 20,000 lymphocyte-gated events, which were then analyzed with CellQuest software (BD Biosciences).

Virus-specific IFN-γ ELISPOT assay

An ELISPOT assay was performed following the method developed by Mothe and Watkins of the Wisconsin University Primate Center (35). Ninety-six-well, flat-bottom plates were coated with anti-IFN-γ mAb (clone MD-1; U-CyTech-BV) and blocked with 2% BSA in PBS. Fresh PBMC were added to the plate at 2×10^5 cells/well in triplicate and then incubated with 0.2 μM pooled SIV Gag peptides (AIDS Research and Reference Program) for 16 h at 37°C. Gold-labeled anti-biotin IgG solution (U-CyTech-BV) was added to the washed plates, which were then incubated for 1 h at 37°C. Individual spot-forming cells (SFC) were counted using the KS ELISPOT compact system (Zeiss) after a 15-min reaction with an activator mix (U-CyTech-BV). An SFC was defined as a large black spot with a fuzzy border (34).

Abs to SIV Gag p27 and SHIV 89.6P Env

SIV Gag- and SHIV Env-specific IgG Ab end-point titers of the macaques' sera were measured by ELISA as previously described (23, 27, 30). All samples were run in triplicate at several dilutions. In brief, 96-well ELISA plates were coated with 0.3 μg of SIV p27 Gag (Advanced Biotechnologies) or 0.2 μM pooled SHIV 89.6P Env peptides (AIDS Research and Reference Program) per well. Heat-inactivated sera were serially diluted, then added to the ELISA plates. Gag- and Env-specific Abs bound to the Ags were captured with alkaline phosphatase-labeled goat anti-mouse IgG (EY Laboratories) and *p*-nitrophenyl-phosphate disodium substrate (Invitrogen Life Technologies).

The SHIV Env-specific neutralization Ab responses induced by challenge with SHIV were analyzed as previously described (28). In brief, 10 μg/ml purified macaque IgG was incubated with 100 50% tissue culture infectious doses ($TCID_{50}$) of SHIV-C2/1, then cultured in M8166 cells. The result was compared with parallel cultures to which preimmune IgG had been added. Neutralization was expressed as the percent inhibition of SIV Gag production in the culture supernatants. Anything >20% of inhibition was considered to be an efficient neutralization response.

Quantitation of plasma viral load

Quantitation of SHIV genomic RNA copies in plasma samples was performed by real-time PCR with a TaqMan assay kit (PerkinElmer Applied Biosystems) and a PRISM 7700 sequence detection system (PerkinElmer Applied Biosystems) as previously described (30). Genomic RNA extracted from plasma samples and SIVmac239 (RNA standard; 5.4×10^4 RNA copies) were subjected to RT-PCR using an SIVmac239–1224 forward, SIVmac239–1326 reverse primer pair and an FAM-SIV-1272T probe. RNA copy numbers from plasma samples were calculated from the standard curve. Data were expressed as RNA copies per milliliter of plasma.

Flow cytometric detection of various subpopulations in CD4$^+$ T cells

Approximately 10^6 fresh PBMC were stained with anti-human CD4 (clone SK3; BD Biosciences), anti-human CD29 (clone 4B4; Beckman Coulter), and anti-human CD45RA (clone 5H9; BD Pharmingen) or with anti-human CD4 (clone *v*-TH/I; Nichirei) and anti-human CD28 (clone KOLT-2, Nichirei). A FACSCalibur (BD Biosciences) was used to acquire 10,000 lymphocyte-gated events, which were then analyzed with CellQuest software.

Statistical analysis

Data are expressed as the mean $\pm$ SD. The data analysis was conducted using the StatView program (SAS Institute), and all reported p values are two-sided. Comparisons between groups were performed using the Kruskal-Wallis H test, followed by the Student-Newman-Keuls correction. Correlations between protection and immune levels were analyzed using Spearman's rank correlation test. A value of $p < 0.05$ was considered significant.

Results

Immunization protocol

Plasmid DNA and the recombinant vaccinia DIs viruses with the inserted *gag/pol* region of SIVmac239 were constructed as previously described (23). Southern blotting confirmed that all plasmids and viruses had the expected genomic structures, whereas Gag-specific Western blots verified the in vitro expression of SIV Gag protein in rDIsSIV*gag/pol*-infected chick embryo fibroblasts (data not shown). In this study we opted to use the three-injection regimen for DNA immunization. Because we found that both the three- and five-injection DNA immunization strategies resulted in similar levels of T cell immunities (23). A total of 19 cynomolgus macaques were divided into four groups (Fig. 1). Group 1 macaques (prime-boost group of five macaques numbered M1 to M5) received three i.m. injections (2.5 mg) of each type of SIV*gag/pol* DNA at 8-wk intervals, followed by two injections of 10^8 PFU of rDIsSIV*gag/pol*. Group 2 macaques (DNA group of five macaques numbered M6, M7, and M14 through M16) received three i.m. injections of the same dose of each type of SIV*gag/pol* DNA at

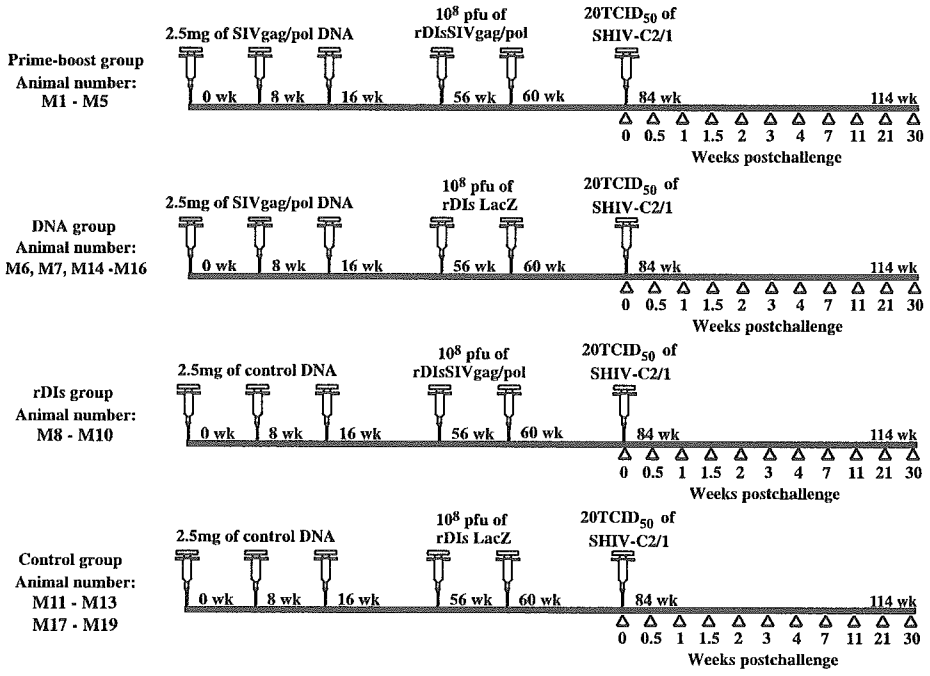

FIGURE 1. Scheme for immunization and viral challenge. Nineteen macaques were divided into four experimental groups and immunized with 2.5 mg of plasmid DNA at weeks 0, 8, and 16, then immunized with 10^8 PFU of rDIs at weeks 56 and 60. Twenty-four weeks after the final immunization, macaques were challenged with 20 $TCID_{50}$ of SHIV.

8-wk intervals, followed by two injections of 10^8 PFU of rDIs-LacZ. Group 3 macaques (rDIs group of three macaques numbered M8 through M10) received three i.m. injections of control DNA pcDNA3.1$^-$ at 8-wk intervals, followed by two injections of 10^8 PFU of rDIsSIV*gag/pol*. Group 4 (control group of six macaques numbered M11 through M13 and M17 through M19) received three i.m. injections of control DNA, followed by two injections of 10^8 PFU of rDIsLacZ. Twenty-four weeks after the second booster inoculation, the macaques were i.v. challenged with 20 $TCID_{50}$ of pathogenic SHIV-C2/1, which were obtained by serum passages of SHIV-89.6. The effects of prime-boost vaccination with DNA and vaccinia DIs on protective immune induction were monitored for 30 wk, then animals were autopsied.

Induction of cellular and humoral immune responses specific for SIV Gag

We first analyzed the induction of cellular immunity by detecting the SIV Gag-specific IFN-γ ELISPOT activities of macaque PBMC after the first and third DNA primings and the first boosting of recombinant DIs in each animal (Fig. 2). A regimen of three consecutive immunizations with SIV*gag/pol* DNA induced 3- to 4-fold higher IFN-γ SFC than did a single immunization in the prime-boost and DNA groups ($p < 0.05$; Fig. 2, *A* and *B*). The numbers of IFN-γ-producing SFC increased ~8- to 9-fold after booster immunization with rDIsSIV*gag/pol* in the prime-boost group ($p < 0.01$; Fig. 2*C*). In contrast, no such increase was seen after booster immunization with rDIsLacZ in the DNA group (Fig. 2*C*). Macaques immunized with control DNA followed by rDIs-SIV*gag/pol* (rDIs group) generated higher IFN-γ SFC than the DNA group ($p < 0.01$; Fig. 2, *B* and *C*). At no point in the course of immunization was Gag-specific IFN-γ SFC detected in the control group. Collectively, our findings show that the DNA/rDIs prime-boost immunization efficiently induced immunodeficiency virus-specific ELISPOT activity in macaques.

To substantiate the induction of cellular immunity specific for SIV Gag, intracellular IFN-γ staining was performed using PBMC after the first booster immunization with rDIs (Fig. 3). Of the four groups tested, the prime-boost group showed the highest frequency of IFN-γ-producing $CD4^+$ and $CD8^+$ T cells. The frequencies of Gag-specific IFN-γ-producing $CD8^+$ and $CD4^+$ T cell responses to Gag peptides in the prime-boost group ranged from 0.51 to 1.22% with an average of 0.82%, and from 0.37 to 0.63% with an average of 0.46%, respectively. The expression of IFN-γ-producing $CD8^+$ and $CD4^+$ T cells immunized with either SIV*gag/pol* DNA (average of $CD8^+$ T cells, 0.095%; average of $CD4^+$ T cells, 0.015%) or rDIsSIV*gag/pol* (average of $CD8^+$ T cells, 0.27%; average of $CD4^+$ T cells, 0.05%) was apparently weak (Fig. 3). Therefore, as observed for the induction of the SIV Gag-specific ELISPOT activities, the prime-boost group proved to be the most efficient of the four animal groups tested at inducing Ag-specific intracellular IFN-γ cytokine staining.

To test for the induction of humoral immunity, we assessed the SIV Gag-specific IgG titers in the animals of each group (Fig. 4). Despite the elevation of Ab titers after the first immunization with SIV*gag/pol* DNA, no enhanced responses were observed after two serial immunizations with the DNA (Fig. 4*A*). However, although the titers did not exceed 2000, enhanced Ab responses were observed after booster immunization with rDIsSIV*gag/pol*. In summary, these results show that the prime-boost vaccine with DNA/rDIs predominantly elicits SIV Gag-specific cellular immune responses in immunized animals.

Enhancement of SIV-specific T cell and humoral immune responses after viral challenge

Twenty-four weeks after the second immunization with rDIs, macaques were challenged with highly pathogenic SHIV. As shown in Fig. 5*A*, Gag-specific IFN-γ SFC levels decreased on the day of challenge in all vaccinated groups, but the increase observed in the numbers of the SFC after SHIV challenge varied among the groups. The most pronounced increase was seen in the prime-boost group, with the average number of Gag-specific IFN-γ-producing cells increasing from 288/million PBMC on the day of challenge to 1124 ($p < 0.01$) 3 days after challenge. The DNA group increased from an average of 104 to 282 ($p < 0.01$), and the rDIs group from 114 to 347 ($p < 0.05$). No significant increases were noted in the control group.

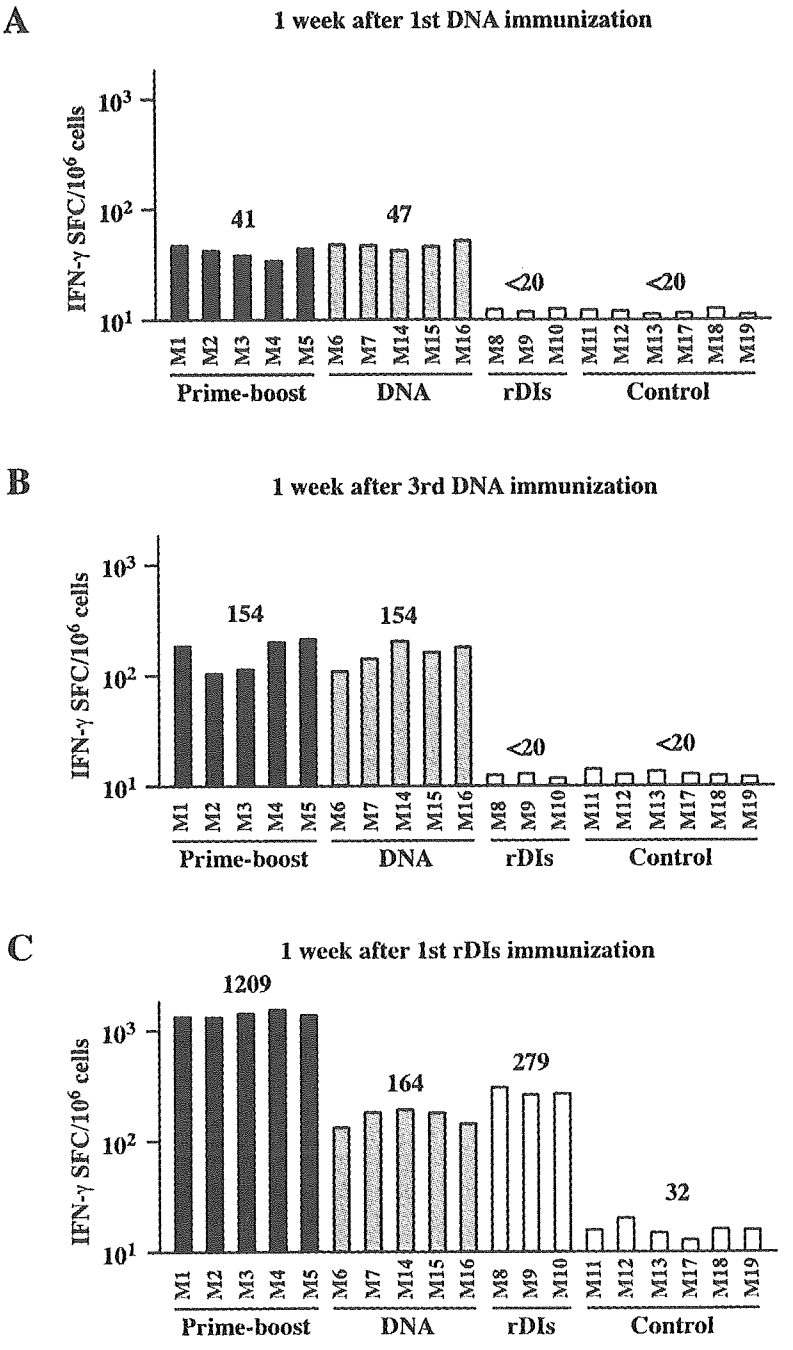

FIGURE 2. Frequency of SIV Gag-specific IFN-γ-producing cells in immunized macaques. Values are provided at 1 wk after the first DNA immunization (*A*), 1 wk after the third DNA immunization (*B*), and 1 wk after rDIs immunization (*C*). The numbers above the data bars represent the geometric means of the SFC levels in each group. Experimental groups and animal numbers are indicated at the bottom of the graph.

Intracellular IFN-γ staining of $CD8^+$ and $CD4^+$ T cells was also performed to assess any enhancement in immunodeficiency virus-specific immune responses (Fig. 5*B*). On the day of challenge, populations of Gag-specific IFN-γ-producing $CD8^+$ T cells in the prime-boost group averaged 0.32%, and populations of $CD4^+$ T cells averaged 0.11%. Three days after viral challenge, the average for Ag-specific IFN-γ-producing $CD8^+$ T cells rose to 0.61%, and that for $CD4^+$ T cells to 0.38%. Gag-specific IFN-γ-producing $CD8^+$ T cells averaged 0.18% for the DNA group and 0.25% for the rDIs group on the day of challenge, with those averages rising to 0.28 and 0.39%, respectively, by 3 days after challenge. Furthermore, the averages for Gag-specific $CD4^+$ T cells in the DNA and rDIs groups rose from 0.08 and 0.10 to 0.14 and 0.23%, respectively. The number of Ag-specific IFN-γ-producing $CD8^+$ and $CD4^+$ T cells in the control group was not affected by viral challenge. Thus, compared with the other three groups of animals, the prime-boost group showed the most significant enhancement of Ag-specific cellular immune responses after viral challenge, suggesting that Gag-specific memory T cell responses may be efficiently generated in animals by immunization with the prime-boost vaccine regimen.

To test the kinetics of humoral immune responses after SHIV challenge, we measured serum IgG titers to SIV Gag and SHIV 89.6P Env in all animals of each group (Fig. 4, *A* and *B*). The SIV Gag-specific IgG titers in all vaccinated animals were rapidly elevated and reached peak levels within 4 wk after challenge (Fig. 4*A*). The peak IgG titers in the prime-boost, DNA, and rDIs groups averaged 14,520 ± 2,508, 5,240 ± 1,099, and 8,400 ± 1,114,

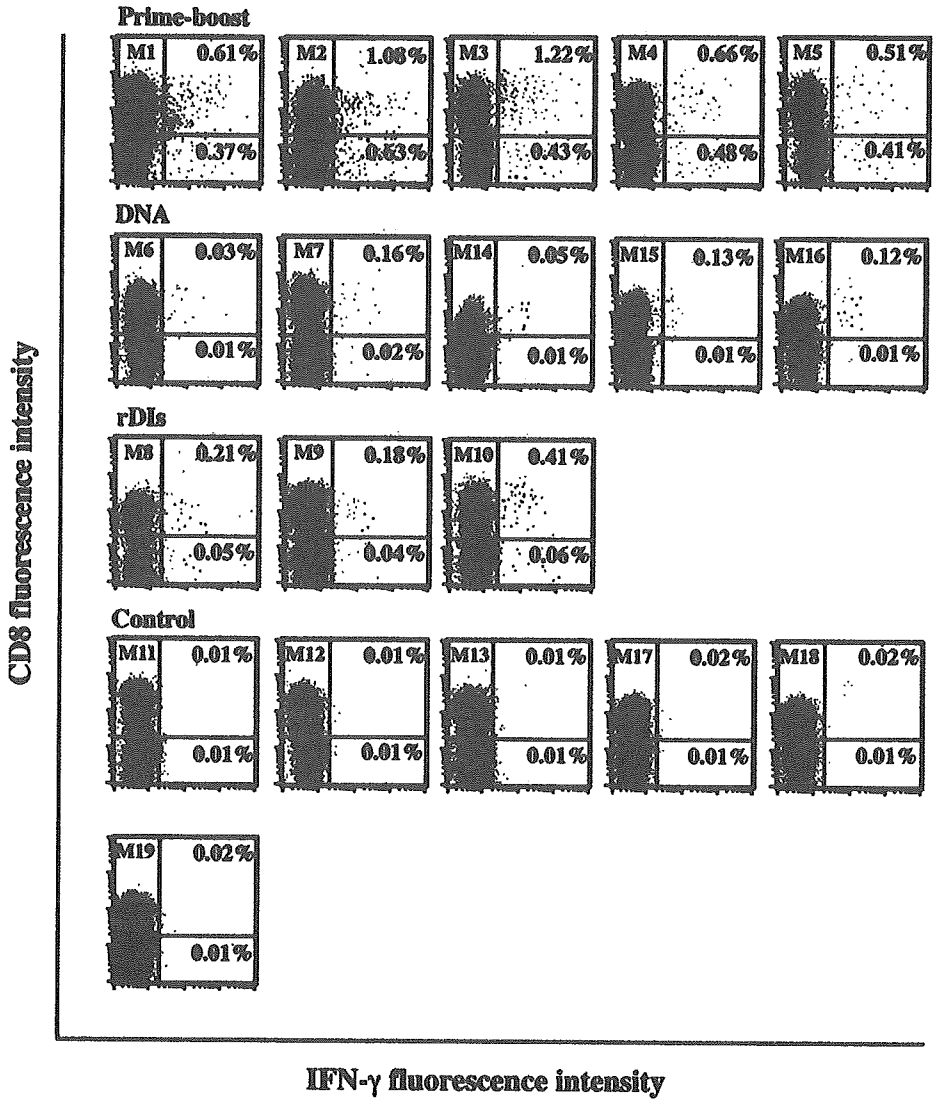

FIGURE 3. Flow cytometric analysis of SIV Gag-specific IFN-γ-producing $CD8^+$ T cells. One week after rDIs boost immunization, freshly isolated PBMC were stimulated with 0.2 μM pooled SIV Gag peptides and stained for anti-CD3, -CD8, and -IFN-γ. Twenty thousand lymphocyte-gated events were acquired. Upper and lower quadrants represent the frequencies of $CD8^+$ IFN-γ^+ and $CD4^+$ IFN-γ^+ T cells, respectively. Numbers indicate the percentage of cells in each quadrant.

respectively, with the increase in the prime-boost group reaching statistical significance ($p < 0.01$), compared with that in the DNA and rDIs groups. The Env-specific IgG appeared by 4 wk after challenge and reached peak levels between 7 and 11 wk. The peak IgG titers in the prime-boost, DNA, and rDIs groups averaged 5,200 ± 1,839, 3,180 ± 701, and 4,533 ± 833, respectively. Both the SIV Gag- and Env-specific IgG titers in the three vaccinated groups maintained high levels and persisted throughout the challenge period. In contrast, no IgG response to Gag and Env was detected in the control group. High titers of Env-specific IgG, but only very low levels of neutralization Ab responses to SHIV-C2/1, were induced in the DNA- and rDI-vaccinated groups (Fig. 4*C*). In contrast, the prime-boost macaques, especially M1, had high levels of neutralization Ab responses (viral neutralization >70%). Thus, these results show that the prime-boost vaccine with DNA/rDIs predominantly elicits SIV Gag-specific humoral responses in immunized animals and generates SHIV Env-specific binding and neutralization Abs after challenge with SHIV.

Macaques of the prime-boost group control plasma viral load and block $CD4^+$-T cell depletion

As noted above, the five macaques in the prime-boost group developed Ag-specific positive immunity after viral challenge. In these macaques, plasma viral loads were most attenuated and $CD4^+$ T cell counts best maintained in peripheral blood (Fig. 6). Peak viral loads occurred 2 wk after challenge in each group. The geometric means of the viral RNA copies were 1.1×10^7 copies in the prime-boost group, 4.7×10^7 copies in the DNA group, 4.1×10^7 copies in the rDIs group, and 4.5×10^7 copies in the control group (Fig. 6*A*). The difference observed in geometric mean peak viremia for the prime-boost and rDIs groups was significant ($p < 0.05$). Levels of peak viremia in the rDIs and control groups did not significantly differ. The peak viral loads in each had decreased by 7 wk after challenge, and the geometric means of the viral RNA copies from 7 to 30 wk were 8.1×10^3 copies (ranging from 7.1×10^3 to 9.4×10^3 copies) in the prime-boost group, 1.1×10^6 copies (ranging from 2.5×10^5 to 6.6×10^6 copies) in the DNA group, 7×10^4 copies (ranging from 5.3×10^4 to 1.1×10^5 copies) in the rDIs group, and 6.8×10^6 copies (ranging from 2.0×10^6 to 5.2×10^7 copies) in the control group (Fig. 6*A*). From 7 to 30 wk, the differences in the geometric means of the viral RNA copies between prime-boost and DNA groups ($p < 0.01$), prime-boost and rDIs groups ($p < 0.01$), and DNA and rDIs groups ($p < 0.01$) vs DNA and control groups ($p < 0.05$) were significant.

Two weeks after challenge, both DNA and control groups showed a serious depletion of $CD4^+$ T cells (to <50 cells) and a corresponding increase in viral RNA. In contrast, the prime-boost

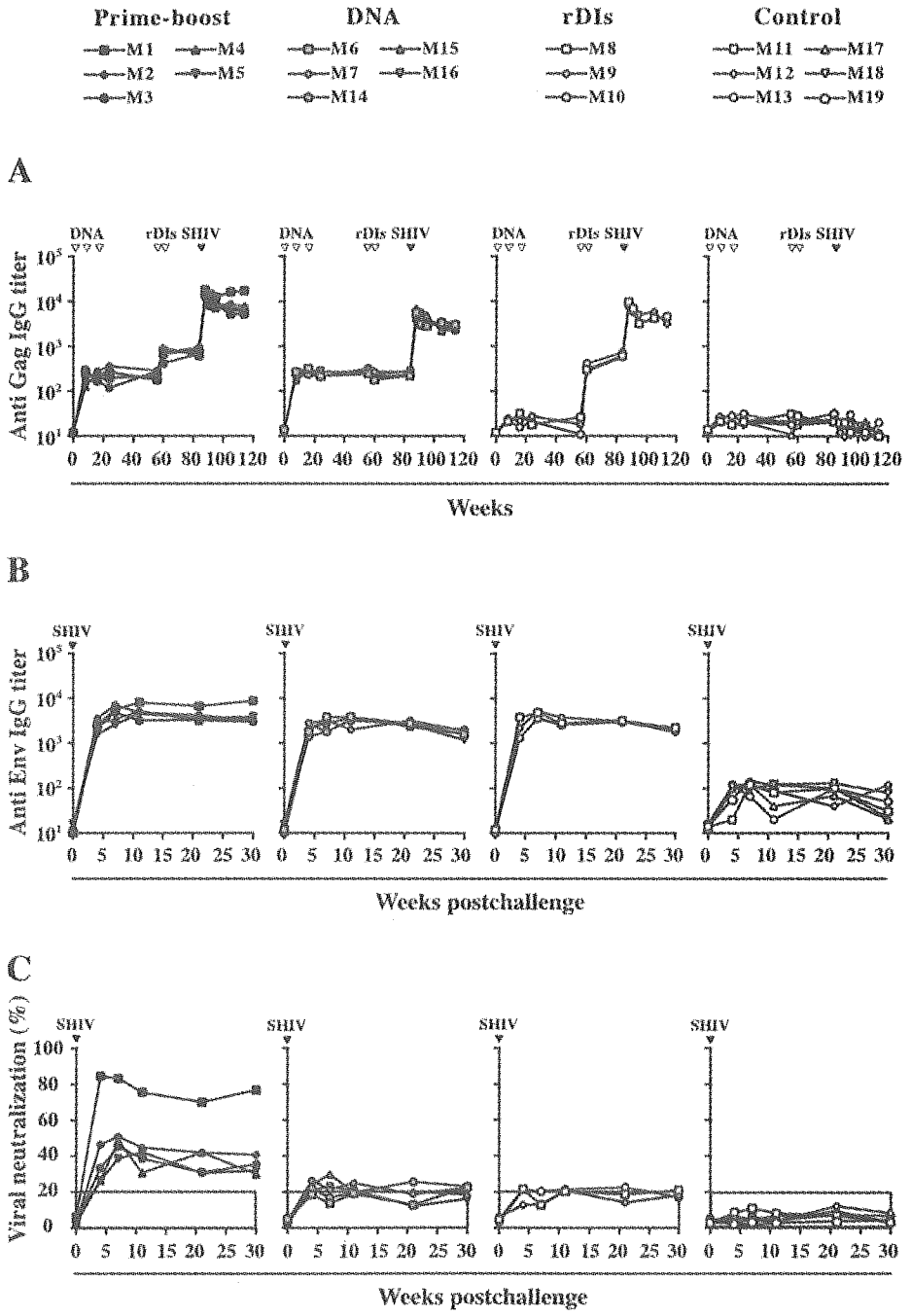

FIGURE 4. Kinetics of serum IgG titers specific to SIV Gag and SHIV 89.6P Env. *A*, SIV p27 Gag- and Env-specific IgG titers after immunization and after challenge. *B*, SHIV 89.6P Env-specific IgG titers. *C*, SHIV-specific neutralization responses. End-point titers of Gag- and Env-specific serum IgG and the percentage of SHIV-specific neutralization responses were measured at each time point. Results represent the average titer and percentage of the average viral neutralization value.

group maintained its $CD4^+$ T cell counts up to 30 wk after challenge (Fig. 6*B*). Four of the five macaques (M2–5) in the prime-boost group exhibited a gradual decrease in $CD4^+$ T cell counts; however, the macaques maintained an average of 254–303 cells from 2 to 30 wk after challenge. The one remaining macaque in the group (M1) maintained an average of 833 $CD4^+$ T cells (ranging from 630 to 1230 cells) and exhibited levels of viral RNA (<500 copies) that were undetectable except when peak viremia was reached at 2 wk (5.7×10^7 copies) and transient viral replication occurred at 7 wk (1.5×10^4 copies; Fig. 6, *A* and *B*).

To characterize the changes in the $CD4^+$ T cell subset in peripheral blood of each group after SHIV challenge, we used flow cytometric analysis to obtain an absolute count and to distinguish among the $CD29^+$, $CD45^+$, and $CD28^+$ cell subpopulations (Fig. 6, *C–E*). By 2 wk after challenge, a sharp decrease in the $CD29^+$ subset of $CD4^+$ T cells was seen in the DNA, rDIs and control groups (Fig. 6*C*). From 2 to 30 wk after challenge, the average number of this subset of cells in the DNA, rDIs, and control groups was 1.21% (ranging from 0.79 to 2.01%), 2.14% (ranging from 1.80 to 3.59%), and 1.03% (ranging from 0.55 to 1.89%), respectively. Similarly, the $CD45RA^+$ subset of $CD4^+$ T cells in the three groups rapidly declined by 2 wk after challenge, with the average of naive cells from 2 to 30 wk being 1.04% (ranging from 0.72 to 1.32%) in the DNA group, 2.83% (ranging from 1.04 to 4.78%) in the rDIs group, and 0.88% (ranging from 0.34 to 1.34%) in the control group (Fig. 6*D*). In contrast, the prime-boost group maintained the highest frequencies of both the $CD29^+$ subset, ranging from 8.0 to 9.63% with an average of 8.82% (Fig. 6*C*), and

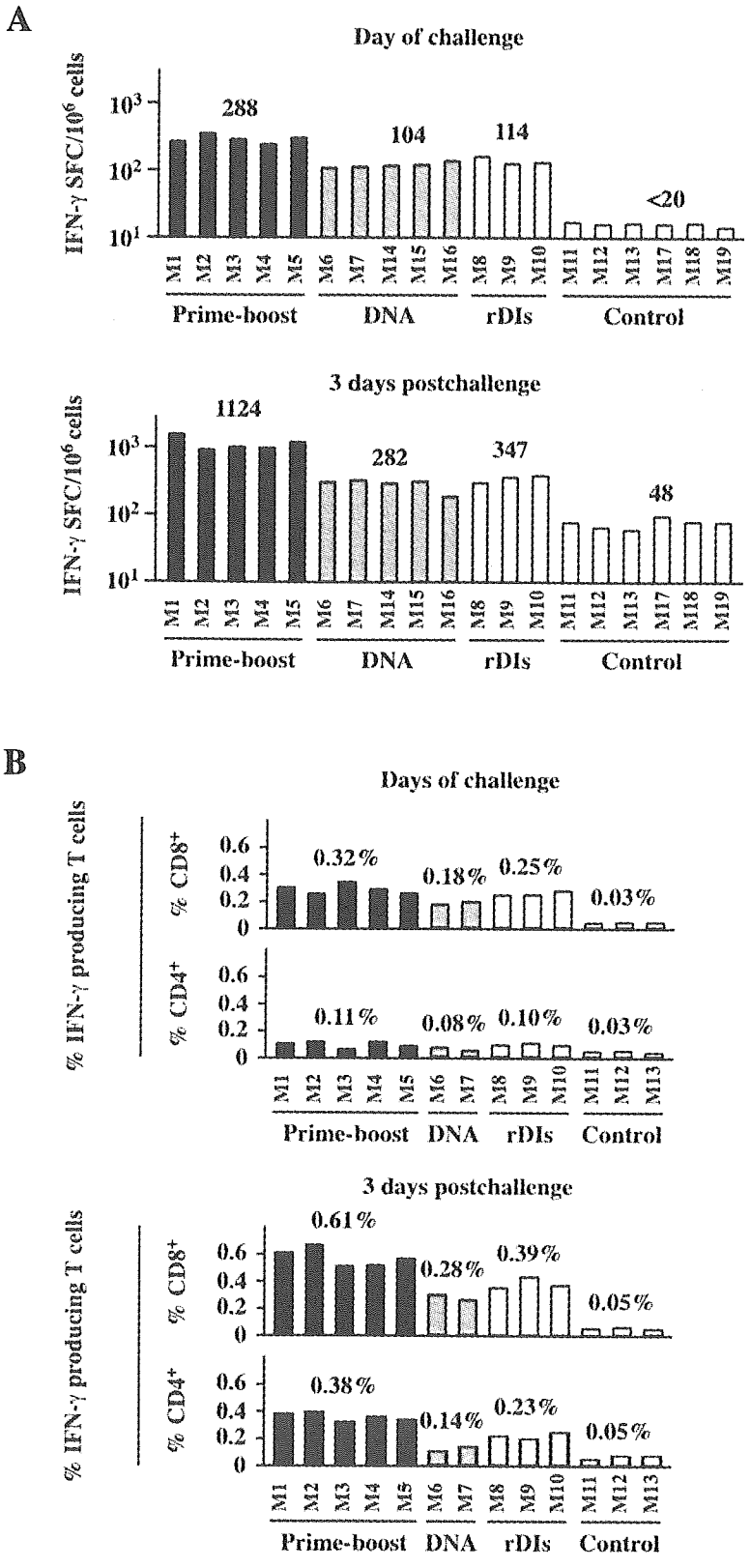

FIGURE 5. Comparison of IFN-γ ELISPOT activity and intracellular IFN-γ-producing T cells specific for SIV Gag in PBMC before and after viral challenge. *A*, ELISPOT activity. The numbers above the data bars represent the geometric means of SFC levels in each group. *B*, Intracellular IFN-γ-producing T cells. On the day of SHIV challenge and 3 days after SHIV challenge, freshly isolated cells were stimulated with SIV Gag peptides and stained for CD3, CD8, and IFN-γ. Numbers represent the percent average of the $CD4^+$ and $CD8^+$ T cell frequencies.

the $CD45^+$ subset, ranging from 6.29 to 9.16% with an average of 7.59% (Fig. 6, *C* and *D*). Flow cytometric analyses also revealed that the number of $CD4^+$ T cells expressing the costimulatory molecule CD28 rapidly dropped in the DNA, rDIs, and control groups by 2 wk after challenge (Fig. 6*E*). The average of $CD4^+CD28^+$ T cells from 2 to 30 wk after challenge in the DNA, rDIs, and control groups was 0.74% (ranging from 0.23 to 1.12%), 1.66% (ranging from 1.01 to 2.6%), and 0.91% (ranging from 0.61 to 1.13%), respectively. In contrast, $CD28^+CD4^+$ T cells in the prime-boost group ranged from 5.27 to 7.26%, with an average of

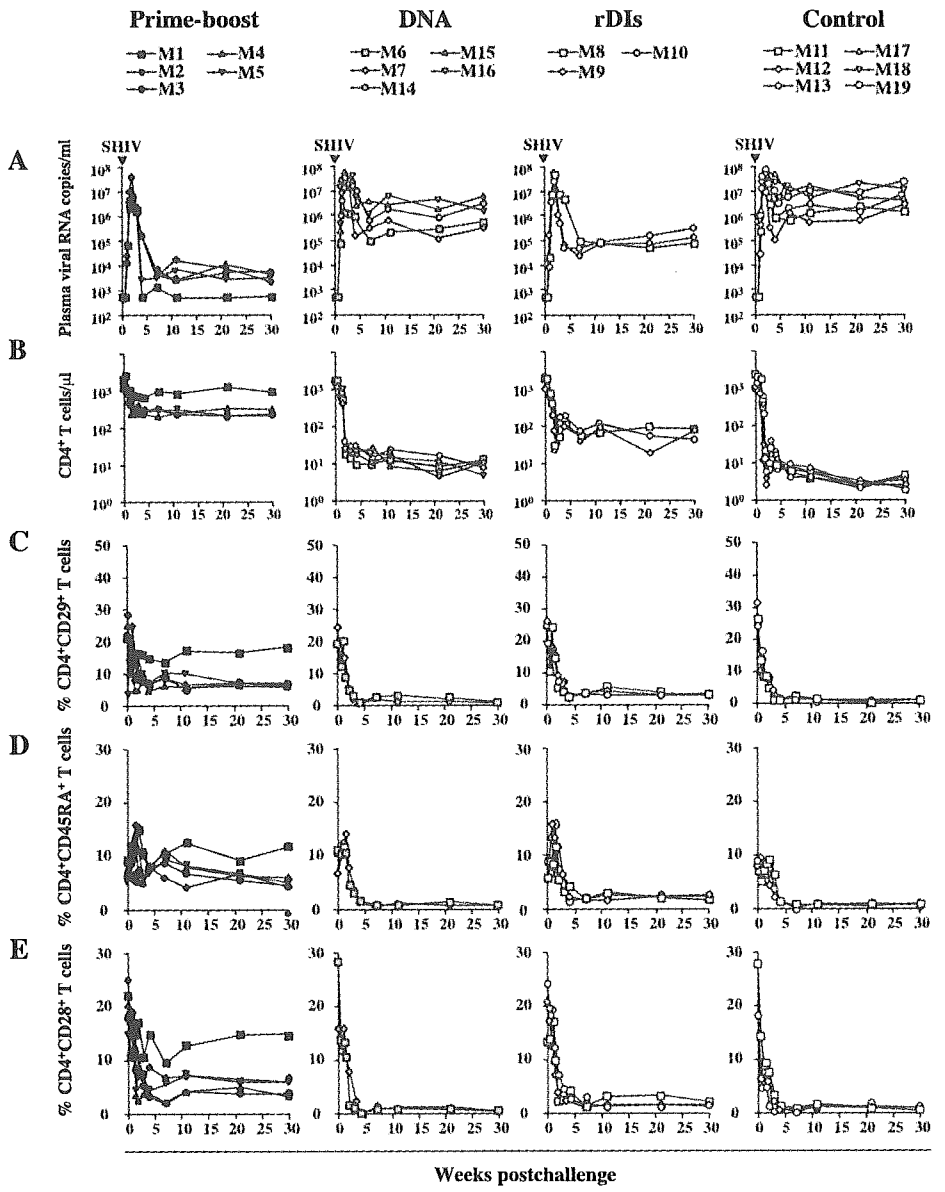

FIGURE 6. Kinetics of viral loads, $CD4^+$ T cell counts, and subpopulations of $CD4^+$ T cells in experimental groups after SHIV challenge. *A*, Plasma viral loads. Plasma viral loads were measured using the real-time PCR system. Levels <500 copies/ml were considered undetectable in this system. *B*, $CD4^+$ T cell counts. Whole blood was stained for CD3, CD4, and CD8 Abs, and $CD4^+$ T cell counts were determined using flow cytometry. *C*, $CD4^+CD29^+$ T cells. *D*, $CD4^+CD45RA^+$ T cells. *E*, $CD4^+CD28^+$ T cells. $CD4^+$ T cell subpopulations were not reduced in the prime-boost animal group.

6.75%. Thus, the prime-boost group maintained $CD29^+$, $CD45RA^+$, and $CD28^+$ cell subpopulations in $CD4^+$ T cells after viral challenge.

Controls of viremia and stability of $CD4^+$ blood lymphocytes correlate with Gag-specific IFN-γ SFC and neutralization Ab responses

Because positive immune responses were detected in the animals immunized with the prime-boost vaccine of DNA/vaccinia DIs, we examined whether any immune responses correlated with the positive immunities using Spearman's rank correlation test (Fig. 7). The set-point levels of plasma viral RNA and $CD4^+$ T cell counts 7 wk after challenge significantly correlated with the Gag-specific IFN-γ SFC levels 3 days after challenge (plasma viral RNA levels vs Gag-specific IFN-γ SFC levels: Rs = 0.850, $p = 4.07 \times 10^{-6}$; $CD4^+$ T cell counts vs Gag-specific IFN-γ SFC levels: Rs = 0.968, $p = 1.10 \times 10^{-11}$; Fig. 7*A*). Interestingly, there was less correlation between the same set-point plasma viral RNA levels and $CD4^+$ T cell counts and the neutralization Ab responses 7 wk after challenge (plasma viral RNA levels vs percent viral neutralization: Rs = 0.796, $p = 4.53 \times 10^{-5}$; $CD4^+$ T cell counts vs percent viral neutralization: Rs = 0.851, $p = 3.93 \times 10^{-6}$). No correlation at all was observed between positive immune responses and anti-Gag and anti-Env Ab titers (data not shown).

Discussion

It is believed likely that HIV-specific immune responses are associated with a decline in viral load and $CD4^+$ T cell maintenance. Our current study using the macaque model suggests that the prime-boost regimen, that is, priming with SIV*gag/pol* DNA followed by boosting with rDIsSIV*gag/pol*, modifies pathogenic SHIV infection. Furthermore, when the relationship between protection and the levels of immune responses was analyzed, we found that Gag-specific IFN-γ T cells showed a strong correlation and neutralization responses a weaker correlation with the suppression of plasma viral RNA levels and maintenance of $CD4^+$ T cell counts. These results accord with previous reports associating

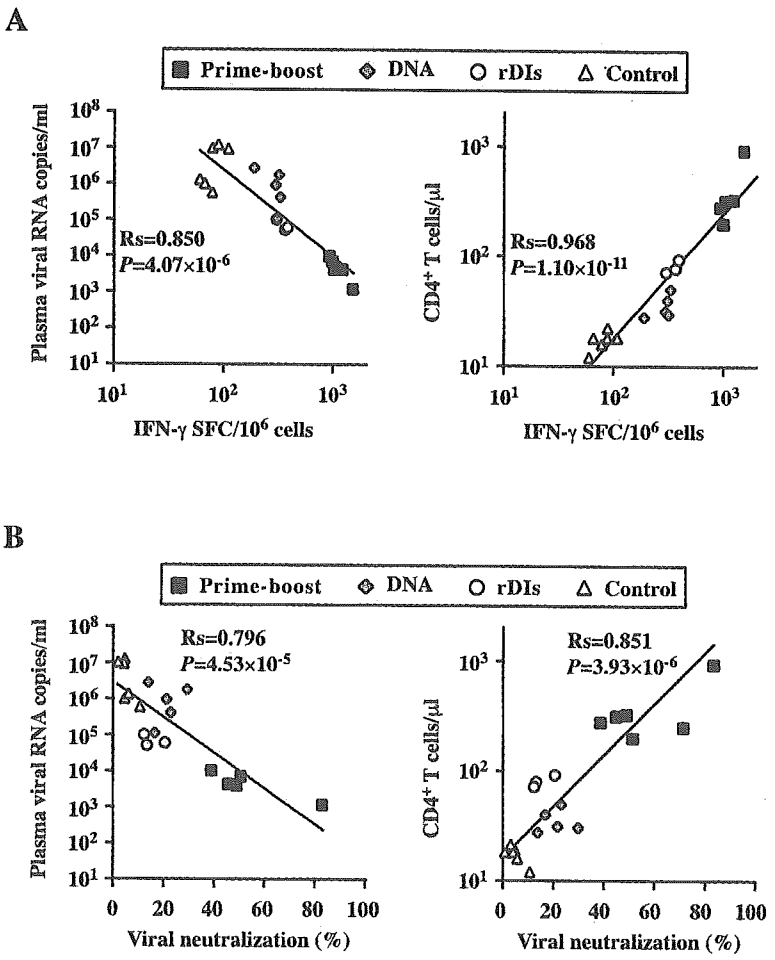

FIGURE 7. Correlations between protection and immune responses. *A*, The correlations between the decline in plasma viral RNA and the increased number of Gag-specific IFN-γ SFC, and between $CD4^+$ T cell counts and Gag-specific IFN-γ SFC. *B*, Correlations between the decline in plasma viral RNA and increased neutralization Ab responses, and between $CD4^+$ T cell counts and neutralization Ab responses. Correlations are calculated using Spearman's rank correlation test.

viral control with cellular immune responses in animals immunized with a prime-boost vaccination of either DNA/MVA (11) or cytokine-augmented DNA (36) encoding *gag* and *env* genes, followed by SHIV challenge. Neutralization Ab production was also detected in the animals (11, 36). Our new observations in vaccine research include the following: 1) Because positive immune responses better correlated with T cell than neutralization responses, it is probable that control of the plasma viral load and $CD4^+$ cell counts was achieved by virus-specific cellular immune responses. 2) Although our vaccine target was only Gag in this strategy, neutralization titers were detected in the prime-boost group that were higher than those induced in animals immunized with DNA, rDIs, or vector controls alone. These higher titers of the neutralization Ab responses against challenge virus might account for the presence of a high number of $CD4^+$ T cells in prime-boost animals (Fig. 6*B*) and might be associated with the production of neutralization Ab. It may, therefore, be reasonable to conclude that anti-Env neutralization Abs were effectively induced in the animals after SHIV challenge. Thus, we suggest that not only cellular responses, but also neutralizing Ab responses, elicited by the challenge virus may play a role in the pathogenesis of HIV/AIDS in the macaque model. 3) This vaccination regimen consisted of DNA and a nonreplicating vaccinia virus DIs, which is very safe even in immunodeficient states. Although other highly attenuated vaccinia strains replicate under synchronized viral infections to mammalian cells (37, 38), the DIs does not replicate in any mammalian cells tested because of natural big deletion of the genome (22, 23, 39). Thus, DIs vaccination eliminates the risk of a disseminated or progressive vaccinia viral infection in the immunocompromised, HIV-infected individual. Therefore, the DNA/DIs vaccine will be most safe in mammalians and may be suitable for therapeutic vaccine.

Recently, we demonstrated that priming with SIV*gag/pol* DNA, followed by boosting with rDIsSIV*gag/pol* generated both Th1-type $CD8^+$ and $CD4^+$ T cell responses specific for SIV Gag, resulting in the protection of immunized mice from a wild-type vaccinia virus recombinant expressing SIV Gag and Pol (23). Our previous mouse and macaque results (23, 40) (Fig. 6) showed that DNA alone was not as effective at inducing positive immunity in the macaque AIDS model as had been reported by others (11, 36). This discrepancy may depend on differences in DNA preparation, for example, whether the target HIV DNA was optimized to the human codon.

Although the exact immune mechanism responsible for protection from viral infection is not yet fully understood, both Ag-specific $CD4^+$ and $CD8^+$ T cell responses were clearly enhanced by viral infection in the prime-boost-immunized animals that exhibited a pronounced attenuation of plasma viral load. Our finding that challenge with the highly pathogenic SHIV virus enhances cellular immunity confirms the results of a recent study (41). It has been demonstrated that HIV-specific $CD8^+$ T cell responses play an important role in controlling viral replication by cytolysis and cytokine and/or anti-virus factor production (1, 2, 3, 42, 43). Others have also documented that HIV-specific $CD4^+$ T cell responses contribute to virus control or the slowing of disease progression (44–46). The critical role played by $CD4^+$ T cell responses against viral infections was also reported in studies of murine

lymphatic choriomeningitis viral infection (47) and CMV immunity in bone marrow transplant recipients (48). DNA/poxvirus prime-boost vaccination induced a high frequency and a high avidity of $CD8^+$ cytotoxic T lymphocyte populations (49), with the magnitude of HIV/SIV-specific $CD4^+$ and/or $CD8^+$ T lymphocyte responses in the course of infection inversely correlating with the viral load (50, 51). In addition, MHC class I molecules loading CTL epitopes may help control viral replication (52–56). The exact mechanisms underlying protective immune responses against HIV-1 remain a subject of debate; however, the above studies suggest that the simultaneous induction after vaccination of both Ag-specific $CD8^+$ and $CD4^+$ T cell responses may make it possible to attenuate immunodeficient viral infection. In this study we showed the efficacy of the prime-boost vaccination by monitoring IFN-γ ELISPOT, intracellular IFN-γ, and Ab responses. In the prime-boost group, boosting with rDIsSIV*gag/pol* induced ELISPOT responses (average of 1209 SFC) almost 10-fold higher than those induced by SIV*gag/pol* DNA (average of 154 SFC). In addition, intracellular IFN-γ staining revealed that the prime-boost vaccination generated high levels of Gag-specific intracellular IFN-γ-producing $CD8^+$ T cells (average, 0.82%; range, 0.51–1.22%) as well. However, lower Gag-specific T cell responses were observed in macaques vaccinated with either SIV*gag/pol* DNA or rDIsSIV*gag/pol* alone than with the prime-boost regimen. In contrast to the strong Gag-specific T cell responses generated by the prime-boost vaccination, humoral responses specific for the same Ag were apparently low throughout the course of immunization. Although the peak IgG titers in the prime-boost group were observed after the first or second boosting with rDIsSIV*gag/pol*, Ab titers remained low. These results are in line with our previous study using the mouse model (23), suggesting that our prime-boost vaccine immunodominantly generates SIV Gag-specific cellular responses in macaques.

Monitoring ELISPOT and intracellular IFN-γ T cell responses specific for Gag revealed that responses decreased at the time of challenge with pathogenic SHIV, but then rapidly recovered. Gag-specific IFN-γ ELISPOT responses in the prime-boost group averaged 288 SFC on the day of challenge and increased to 1124 SFC on day 3 after challenge. The population of intracellular IFN-γ-producing $CD8^+$ and $CD4^+$ T cells specific for Gag also increased from an average of 0.32 to 0.61% and from an average of 0.11 to 0.38%, respectively, suggesting that our prime-boost vaccine generated a high frequency of very responsive $CD4^+$ and $CD8^+$ memory T cells that immediately reactivated sufficient levels of the Ag-specific immune responses against the SHIV Ag. Furthermore, a kinetic study of plasma viral loads and counts of $CD4^+$ T cells after challenge with SHIV revealed different patterns for each group. Although peak plasma viral loads were observed 2 wk after challenge in all groups, the number of plasma RNA copies peaking at that time in the prime-boost group were ~5-fold lower than in other groups, with numbers remaining depressed during the period extending from 7 to 30 wk after infection. However, high $CD4^+$ T cell counts were maintained in the prime-boost group. These results suggest a correlation between both plasma viral loads and the maintenance of high $CD4^+$ T cell counts and T cell response levels.

With regard to safety of vaccinia DIs as a vaccine vector, its viral replication occurs only in chick embryo fibroblasts, not in any mammalian cell lines tested (22, 24–26, 57). Because a vaccine regimen combining DNA and a defective DIs vector would not run the risk that the virus used as vector might replicate and disseminate, it would pose less of a risk to a severely immunocompromised host. Furthermore, in this study using the macaque model, we demonstrated that the cellular immune responses generated by the prime-boost vaccination were higher than those induced by vaccination with either DNA or rDIs alone and that response levels correlated to plasma viral loads and $CD4^+$ T cell counts after challenge with pathogenic SHIV. In summary, these results demonstrate that the new prime-boost regimen safely and effectively elicits anti-immunodeficiency viral immunity, suggesting its promise as a potential vaccine against HIV-1 infection as well as against HIV-induced disease progression.

Current macaque models of HIV, SIV, and SHIV may fall short of precisely mirroring human HIV infection. In some macaque HIV/AIDS models, SIVmac239 has been targeted as a desirable challenge virus, because it is a typical CCR5-tropic SIVmac and can cause both chronic and progressive disease in macaques (41, 58, 59). However, the virus is very difficult to neutralize and also very difficult to clear even from animals that have been previously immunized with homologous recombinant vector-based vaccines (41, 58, 59). Only live attenuated SIV has been reported to control SIVmac239 (T. Allen, Global HIV Vaccine Enterprise Meeting, Washington, October 21, 2004). Although there may be no macaque model suitable for evaluating the efficacy of an SIV or HIV experimental immunogen, in this study we clearly showed that vaccination with an SIV experimental immunogen consisting of SIV*gag/pol* DNA and replication-defective rDIsSIV*gag/pol* caused a pronounced attenuation of the infection caused by a highly pathogenic variant of SHIV-C2/1 in all five macaques tested. SHIV-C2/1, used as challenge virus, is a variant of SHIV 89.6. Because SHIV89.6 does not induce both a marked decline in $CD4^+$ cells and a high level of plasma viral load in cynomolgus macaques, we passaged serum from virus-infected cynomolgus macaques. The variant was obtained by the serum passages using cynomolgus macaques inoculated with SHIV89.6, and it induced high levels of viremia ($1–10 \times 10^7$ viral RNA copies/ml) and marked $CD4^+$ T cell depletion (<10 cells/μl) within 2 and 3 wk after viral inoculation (30, 31, 39). Furthermore, genomic study revealed 16 mutations of genomic DNA and 15 amino acid mutations in the Env region of parental virus. Thus, the cynomolgus AIDS model challenged with SHIV-C2/1 may represent primary HIV-1 infection in humans. These results should prove useful in determining how potent the new prime-boost vaccine regimen might be at eliciting anti-immunodeficiency virus immunity.

HIV-1 has been reported to preferentially infect $CD45RO^+CD4^+$ T cells in the early stages of infection, with the number of $CD45RA^+CD4^+$ T cells declining in later stages (60–62). Furthermore, the loss of this subpopulation of $CD4^+$ T cells during the early phase of immunodeficiency virus infection correlates to disease progression (63, 64), whereas the low $CD45RA^+CD4^+$ T cell levels in the late stages of infection correlate with an increased risk of death (65–67). The levels of $CD4^+$ T cells expressing the $CD28^+$ molecule have also been demonstrated to correlate with disease progression (68, 69). To confirm the effect of prime-boost immunity after SHIV challenge, we analyzed the kinetics of $CD4^+$ T cells expressing $CD29^+$, $CD45RA^+$, and $CD28^+$ molecules. We observed that the prime-boost group maintained the subpopulations of $CD4^+$ T cells throughout the course of infection, with an average of 8.82% $CD29^+$ cells, 7.59% CD45 RA^+ cells, and 6.75% $CD28^+$ cells. In contrast, $CD4^+$ T cell populations in the other DNA and rDIs groups were reduced to <3%. These results suggest that immunization with the new prime-boost regimen induces protective immunity while maintaining the levels of the various $CD4^+$ T cell subpopulations.

In summary, our study has shown that the vaccine strategy that primes with DNA and then boosts with the replication-defective